Limnol. Oceanogr., 54(1), 2009, 289–308

Variability of *Pseudo-nitzschia* and domoic acid in the Juan de Fuca eddy region and its adjacent shelves

Vera L. Trainer[1]
National Oceanic and Atmospheric Administration, Northwest Fisheries Science Center, Seattle, Washington 98112

Barbara M. Hickey, and Evelyn J. Lessard
School of Oceanography, University of Washington, Seattle, Washington 98195

William P. Cochlan
Romberg Tiburon Center for Environmental Studies, San Francisco State University, Tiburon, California 94920

Charles G. Trick
The Schulich School of Medicine and Dentistry, Departments of Biology, Microbiology and Immunology, The University of Western Ontario, London, Ontario N6A 5B7, Canada

Mark L. Wells
School of Marine Sciences, University of Maine, Orono, Maine 04469

Amoreena MacFadyen, and Stephanie K. Moore[2]
School of Oceanography, University of Washington, Seattle, Washington 98195

Abstract

The Juan de Fuca eddy is a toxic "hot spot." Domoic acid (DA) was detected in the eddy during each of six cruises over a 4-yr study, although *Pseudo-nitzschia* abundance and toxin concentrations were highly variable. During the September 2004 eddy bloom, *Pseudo-nitzschia* spp. exceeded 13×10^6 cells L^{-1}, and particulate DA reached 80 nmol L^{-1}. Of the >10 species of *Pseudo-nitzschia* identified in this region, those coincident with the most toxic blooms are *P.* cf. *pseudodelicatissima*, *P. cuspidata*, *P. multiseries*, and *P. australis*. However, the presence of any particular species could not be used as an indicator of toxicity because of the high level of variability in intracellular DA in field assemblages. *Pseudo-nitzschia* cells were typically associated with blooms of other diatom taxa but also were coincident with blooms of euglenoids and dinoflagellates in the eddy region. *Pseudo-nitzschia* always comprised <17% of the total carbon biomass, thereby rendering remote sensing an unsuitable means for predicting toxigenic *Pseudo-nitzschia* blooms in this region. Our results support the hypothesis that the Juan de Fuca eddy region and not the nearshore zone is the primary initiation site for toxic blooms of *Pseudo-nitzschia* affecting the Washington coast. Although particulate DA was observed near the edges of the Columbia River plume, whether toxin can be produced in situ in plume water is not resolved. No first-order predictive relationships were found for either *Pseudo-nitzschia* abundance or DA concentration and environmental data from all six cruises.

[1] Corresponding author (Vera.L.Trainer@noaa.gov).
[2] Present address: National Oceanic and Atmospheric Administration, Northwest Fisheries Science Center, Seattle, Washington 98112.

Acknowledgments

We thank the officers and crew of the R/V *Wecoma*, R/V *Atlantis*, R/V *Thompson*, and R/V *Melville* for their assistance. We thank J. Herndon for nutrient analysis; N. Tsui, B. Bill, and A. Odell for the *Pseudo-nitzschia* cell enumeration; K. Baugh and S. Nance for DA analyses; M. Bernhardt and M. Foy for plankton analyses; M. Auro, R. Radan, and N. Ladizinsky for pigment analyses; N. Kachel for conductivity, temperature, depth (CTD) analyses; S. Geier and numerous other colleagues for cruise support; and N. Adams and S. Day for assistance with the figures. We gratefully acknowledge N. Lundholm, C. Stehr, and B. Bill for electron microscopy; R. Stumpf and M. Tomlinson for satellite imagery; and two anonymous reviewers for their comments on this manuscript. The Ecology and Oceanography in the Pacific Northwest (ECOHAB-PNW) project was funded by the National Science Foundation's (NSF) ECOHAB project OCE-0234587 and NOAA ECOHAB grant NA16OP1450. This is ECOHAB publication 266 and ECOHAB-PNW publication 18.

Domoic acid (DA), produced by species of the diatom genus *Pseudo-nitzschia*, was first recognized as a biotoxin to humans when over 100 people became severely ill after consuming mussels harvested near Prince Edward Island, Canada, in 1987 (Wright et al. 1989). Most of the known toxic events in North America since that time have occurred on the U.S. West Coast, where DA was first implicated in the illness and death of brown pelicans and Brandt's cormorants in Monterey Bay, California, in 1991 (Work et al. 1993). In October 1991, about 1 month following the toxic bloom of *Pseudo-nitzschia* in California, DA concentrations above the regulatory limit were found in the edible parts of Pacific razor clams (*Siliqua patula*) and Dungeness crabs (*Cancer magister*) on the Washington coast (Wekell et al. 1994). In 1998, the deleterious effect of DA on the health of marine mammals, in particular, California sea lions (*Zalophus californianus*), was confirmed for the first time along the West Coast (Scholin et al. 2000),

although these poisoning events are now believed to have had a historical precedence.

Production of DA by *Pseudo-nitzschia* spp. is not constitutive. Toxin production tends to be lost in cells during prolonged periods in culture (Baugh et al. 2006). A variety of culture studies with different isolates of *Pseudo-nitzschia* have suggested that the DA production occurs as a stress response to limiting macronutrients (Bates et al. 1991; Pan et al. 1996*a*,*b*) and/or micronutrients (Rue and Bruland 2001; Maldonado et al. 2002; Wells et al. 2005), elevated pH (Lundholm et al. 2004), and, most recently, the form of nitrogen available for growth (Howard et al. 2007).

Washington State razor clam fisheries have been subject to repeated closures in recent years because of DA occurrence. In particular, selective beaches have been closed to shellfish collection in 1991, 1993, and every year from 2000 to 2006 (Trainer and Suddleson 2005; Washington State Department of Health 2007). Coastwide closures have greatly reduced the harvest potential of the razor clam fishery in 1992, 1998, 1999, 2002, and 2003, and recreational and commercial harvesting of Dungeness crabs were prohibited in early 2003. Aside from human health-related issues, these toxic events translate into millions of dollars of annual economic losses in this region alone.

A quasi-permanent cyclonic eddy off the mouth of the Strait of Juan de Fuca, termed the ''Juan de Fuca'' or ''Tully'' eddy, has been observed frequently to contain significant *Pseudo-nitzschia* populations. It is hypothesized that the eddy is an initiation site for toxic blooms of the *Pseudo-nitzschia* cells responsible for razor clam toxification on Washington State beaches (Adams et al. 2000; Trainer et al. 2001, 2002). This seasonal, topographically linked feature develops near the time of the spring transition and declines during the fall (Freeland and Denman 1982). During spring and summer, along-shelf winds typically blow from the northwest and force a seasonal-mean, southeastward-flowing, baroclinic current over the slope and outer shelf. However, during storm events when the winds reverse and blow from the southwest, observational and modeling studies have shown that these downwelling-favorable conditions can transport particles streaming southward from the eddy to the inner Washington shelf (MacFadyen et al. 2005). The coastwide closure of the Washington razor clam fishery in 1998 followed a late summer storm (Adams et al. 2000; Trainer et al. 2002), consistent with the hypothesis that toxigenic *Pseudo-nitzschia* cells can be transported to the coast from offshore locations.

Other areas on the U.S. West Coast also have been recognized as important in *Pseudo-nitzschia* bloom dynamics, including coastal waters near Point Conception, Point Año Nuevo, and the Farallon Islands, California, and Heceta Bank, off the central Oregon coast (Trainer et al. 2000, 2002). These areas have some physical features that bear some resemblance to the Juan de Fuca eddy. For example, in these regions, flow–topography interactions can lead to enhanced surface plankton retention, as seen in the Juan de Fuca eddy, in contrast to the open regions of Eastern Boundary Upwelling Systems that are characterized by long and straight coastlines (Hickey and Banas 2003).

Motivated by the perceived relationship between DA production and plankton-retentive coastal sites and also by the demonstrated physical pathway between the Juan de Fuca eddy and coastal clamming beaches, the Ecology and Oceanography of Harmful Algal Blooms in the Pacific Northwest (ECOHAB-PNW) program was designed to determine (1) whether the Juan de Fuca eddy is a persistent initiation site for toxigenic diatom blooms that affect the adjacent and southern coastal beaches; (2) if so, under what environmental and chemical conditions this occurs; and (3) whether toxic blooms also can initiate in the nearshore coastal upwelling zone. The long-term program goal was to characterize the environmental factors leading to toxic bloom formation with sufficient accuracy to provide early warning of bloom events that affect the Washington coast.

ECOHAB-PNW included both physical and biological modeling, in situ field observations, and experimental studies over 4 yr by an interdisciplinary research team. In situ observations included at-sea data collection on a regional sampling grid, moored sensor arrays, satellite data and surface drifter deployments, and studies of the temporal evolution of blooms tracked by drifters. At-sea data collections included information on phytoplankton community structure, growth and grazing rates (Olson et al. 2006, 2008), nutrients (including iron), hydrographic information (MacFadyen et al. 2008), and shipboard current profiles. Deckboard incubation studies using natural assemblages of phytoplankton, including *Pseudo-nitzschia*, were performed to determine the biological controls most essential to successful growth and toxin production by *Pseudo-nitzschia*. Modeling studies using data from the 4 yr of ECOHAB-PNW cruises (Foreman et al. 2008) have shown that the Juan de Fuca eddy is formed seasonally as a result of the interaction of the southward upwelling jet with strong, topographically linked upwelling off Cape Flattery and the buoyant outflow from the Strait of Juan de Fuca. MacFadyen et al. (2008) describe the physical oceanographic setting of the ECOHAB-PNW cruises. In particular, they address the physical and chemical conditions favorable for development of phytoplankton blooms in the Juan de Fuca eddy region as well as the subsequent escape of cells from the eddy and transport toward the coast.

Here we compare the distributional patterns of *Pseudo-nitzschia* abundance and species as well as DA concentrations from six cruises with physical forcing, community assemblages, and dissolved nutrient patterns and supply. The findings are used to address specific ECOHAB-PNW objectives: determining whether the eddy region and/or the nearshore zone are initiation sites for toxic blooms, which species are responsible, and whether blooms are related to the occurrence of macronutrient stress or specific phytoplankton community assemblages. Research results that address objectives pertaining to the physical processes that control eddy generation, retentiveness, and transport of toxigenic cells from the eddy to the coast are detailed elsewhere (MacFadyen et al. 2005, 2008; Foreman et al. 2008).

Methods

Cruises—Cruises occurred in both summer and fall over a 4-yr period, with more frequent sampling conducted in the fall because of the historically common toxic events on coastal beaches at that time. Cruises were conducted 02–23 June 2003 and 30 August–19 September 2003 aboard the R/V *Wecoma*, 08–28 September 2004 and 07–27 July 2005 aboard the R/V *Atlantis*, 02–22 September 2005 aboard the R/V *Melville*, and 11 September–04 October 2006 aboard the R/V *Thompson*. The ECOHAB-PNW survey grid encompassed areas off the coasts of southern Vancouver Island, British Columbia, Canada (as far north as Barkley Sound), and Washington coast, USA (as far south as Grays Harbor [GH]), and included both the Juan de Fuca eddy and the mouth of the Strait of Juan de Fuca (Fig. 1a). During each of the six cruises, the grid was surveyed over a continuous 6–10-d period (Fig. 1b). Selected transect lines or portions of the grid were resampled if wind conditions changed significantly during the cruise. Data from the 6–10-d grid plus additional partial surveys during a given cruise are collectively referred to as 21-d cruise data (Table 1c). Data are described as originating from the "eddy region," the "filament zone," which is the region downstream of the eddy where high chlorophyll *a* (Chl *a*) filaments have been observed, and the "nearshore zone," the region in which coastal upwelling sometimes occurs (Fig. 1a).

Hydrographic data—Continuous vertical profiles were collected using a Sea-Bird Electronics (SBE) 911 plus conductivity, temperature, and depth system with dual temperature and conductivity sensors attached to a rosette equipped with 10-liter polyvinyl chloride Niskin bottles. Processing included the use of standard Sea-Bird software, comparison of data from primary and secondary sensors, comparison of pre- and postcruise calibrations, and, in the case of salinity, comparison with bottle samples. Discrete seawater samples were collected routinely from depths of 1, 5, and 10 m (and from depths of 15, 30, 50, 100, 200, and 500 m and 5 m off the bottom at selected stations) and analyzed onboard for nutrients, Chl *a*, DA, and *Pseudo-nitzschia* identification and enumeration as described here.

Pseudo-nitzschia *counts and species determination*—Samples were collected during grid surveys at 1-, 5-, and 10-m depths. Total *Pseudo-nitzschia* cells were quantified from whole water samples preserved with buffered formalin (<1% final concentration). Cells were enumerated with a Palmer-Maloney counting chamber using a Zeiss Axiovert 135 inverted light microscope. Samples (50 mL) were settled when necessary for at least 24 h and counted at 200× (total) magnification. Surface phytoplankton samples were collected for *Pseudo-nitzschia* species identification at each station using a 20-μm mesh phytoplankton net. The relative contribution of each *Pseudo-nitzschia* species to the total *Pseudo-nitzschia* cell abundances were determined on ~10% of the full grid surface stations by scanning electron microscopy (SEM) of net tow samples using the method described in Bill et al. (2006). *P. cuspidata* were positively

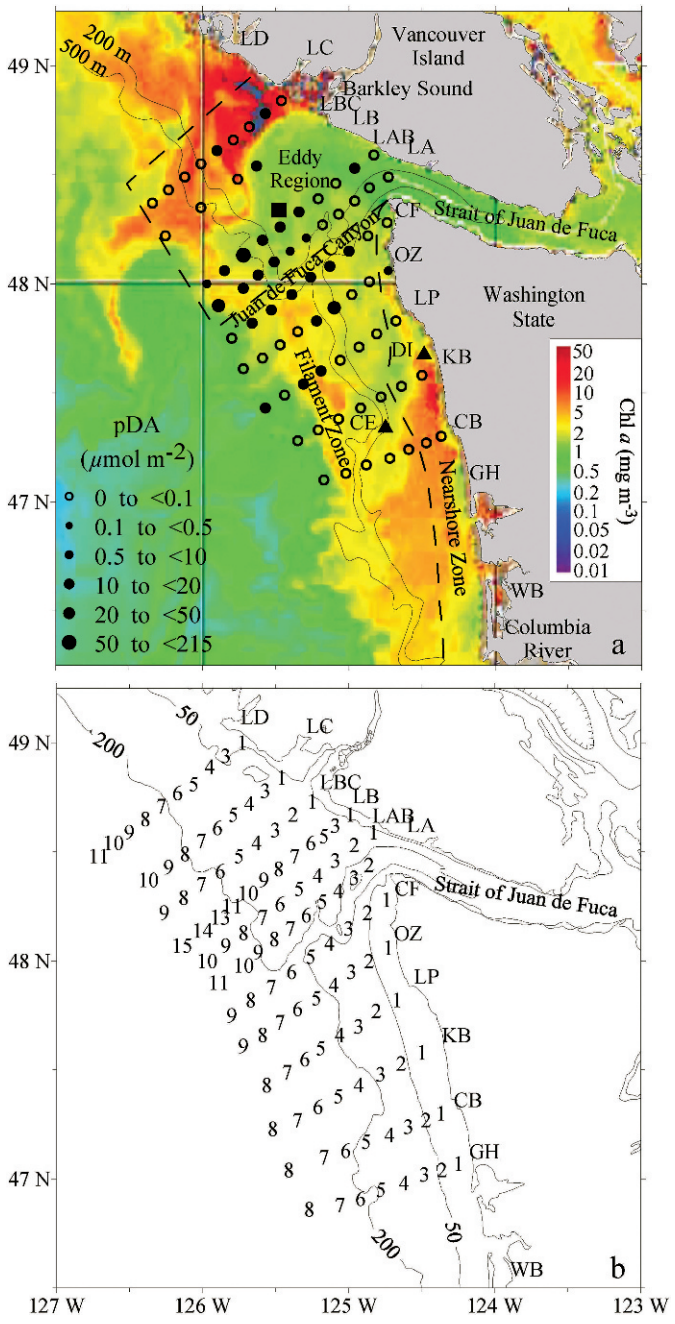

Fig. 1. (a) Integrated pDA concentrations (μmol m^{-2}) for 1, 5, and 10 m at each station during the ECOHAB-PNW grid survey, shown together with SeaWiFS satellite imagery of Chl *a* concentration from 02 September 2003. Integrated concentrations were determined by trapezoidal integration (*see* text for details). The limit of detection for pDA was 0.1 nmol L^{-1}. The eddy, filament, and nearshore zones are delineated by dashed lines. The Cape Elizabeth (CE) and Destruction Island (DI) wind stations are shown as solid triangles, and the location of moored surface current measurements is shown as a solid square. The satellite image was from a clear day during the complete survey (01–06 September). Poor weather prevented sampling of all stations on the grid survey. (b) Stations in the sampling plan for all six ECOHAB-PNW cruises. During the September 2003 cruise depicted here, the grid was sampled from south to north. ECOHAB-PNW grid stations (numbered) and transect lines (lettered) are shown with 50- and 200-m bathymetry.

Table 1. Stations with detectable *Pseudo-nitzschia* and pDA at (a) 1-m depth; (b) 1-, 5-, and 10-m depths during the 6–10-d grid surveys; and (c) 1-, 5-, and 10-m depths during the 21-d cruises.

Date	*Pseudo-nitzschia** (%)	pDA† (%)	*Pseudo-nitzschia* in nearshore (%)	*Pseudo-nitzschia* in eddy (%)	pDA in nearshore‡ (%)	pDA in the eddy region§ (%)
a. Grid: 1 m						
Jun 2003	54	2	7	34	2	0
	n=84‖	n=88				
Sep 2003	96	28	9	43	1	18
	n=74	n=74				
Sep 2004	72	65	6	40	7	35
	n=97	n=97				
Jul 2005	45	7	6	28	0	7
	n=99	n=99				
Sep 2005	45	20	9	11	5	4
	n=104	n=97				
Sep 2006	36	1	6	18	0	0
	n=108	n=108				
b. Grid: 1, 5, 10 m						
Jun 2003	54	4	7	35	2	2
	n=85	n=89				
Sep 2003	96	38	9	43	1	22
	n=74	n=74				
Sep 2004	84	78	6	48	8	41
	n=97	n=97				
Jul 2005	45	20	6	28	3	15
	n=99	n=99				
Sep 2005	47	29	9	12	5	9
	n=104	n=97				
Sep 2006	41	3	7	20	0	1
	n=108	n=108				
c. 21-d cruises: 1, 5, 10 m						
Jun 2003	78	34	8	49	4	25
	n=88	n=89				
Sep 2003	91	48	9	44	5	23
	n=98	n=98				
Sep 2004	90	87	6	50	8	44
	n=97	n=97				
Jul 2005	46	27	6	28	5	16
	n=110	n=110				
Sep 2005	50	28	8	15	6	9
	n=107	n=107				
Sep 2006	50	3	8	20	0	1
	n=117	n=117				

* Limit of detection is 1000 cells L^{-1}.
† Limit of detection is 0.1 nmol L^{-1}.
‡ Percentage of stations with detectable pDA at the coast. Nearshore stations are defined as CF1, OZ1, LP1, KB1, KB2, CB1, CB2, GH1, GH2, WB1, and WB2 (n = 11; *see* Fig. 1).
§ Percentage of stations with detectable pDA in the eddy. The eddy region is defined as all stations on lines LA to LD (n = 61; *see* Fig. 1).
‖ n = number of stations sampled; n = 1 for any given station even when multiple depths were sampled.

identified in samples from the September 2004 and 2005 cruises using transmission electron microscopy (Lundholm et al. 2003).

As electron microscopy could not be performed on every sample, *Pseudo-nitzschia* cells were grouped into the three size categories of *pseudodelicatissima/delicatissima/cuspidata* (p/d/c), *australis/fraudulenta/heimii* (a/f/h), and *pungens/multiseries* (p/m) using light microscopy (Trainer and Suddleson 2005). Samples chosen for SEM were representative of the major species groupings found in the eddy, filament, or nearshore zones (outlined in Fig. 1a) during each grid survey. When possible, stations were chosen for SEM analysis where at least 50 *Pseudo-nitzschia* cells could be viewed, though DA was not necessarily detectable.

Phytoplankton community composition and biomass—Separate water samples were collected for analysis of total phytoplankton community composition and biomass estimations. To identify, enumerate, and size all phytoplankton cells, samples were preserved with glutaraldehyde (0.5% final concentration) and acid Lugol's (5% final concentration). Within a few hours of collection, aliquots of the glutaraldehyde-fixed samples were stained with 4′,6-diamidino-2-phenylindole and proflavin and filtered onto

0.2- and 0.8-μm black polycarbonate (GE Osmonics) filters (Lessard and Murrell 1996). The filters were mounted on slides with low fluorescence immersion oil and stored frozen for analysis onshore. Picophytoplankton (<2 μm) and nanophytoplankton (<10 μm) cells were counted on the 0.2-μm filters at 1000× and microphytoplankton (>10 μm) on the 0.8-μm filters at 400× on a Zeiss Standard epifluorescence microscope. *Pseudo-nitzschia* cells were counted and sized in the glutaraldehyde-fixed samples at 400× magnification. Larger, more rare diatoms and dinoflagellates were enumerated and sized from settled Lugol's samples at 250× with a Zeiss inverted microscope. Picoplankton (cyanobacteria and picoeukaryotes) were sized using images taken with a QImaging Retiga EX charged coupled device camera and Image Pro Plus software. All other groups were sized (including *Pseudo-nitzschia*) using a computer-aided digitizing system (Roff and Hopcroft 1986). Cell volumes and carbon were calculated using appropriate geometric equations reported in Menden-Deuer and Lessard (2000) for diatoms, nanophytoplankton, and dinoflagellates and in Worden et al. (2004) for picoplankton. For *Pseudo-nitzschia* biomass determinations, cells were separated into two size categories based on the width of the cell valve. *Pseudo-nitzschia* spp. with a transapical axis narrower than 3 μm were categorized as small cells; this grouping includes *P. cuspidata* and *P. pseudodelicatissima/delicatissima*. Cells with a transapical axis wider than 3 μm were classified as large cells; this group includes *P. australis*, *P. fraudulenta*, *P. heimii*, *P. pungens*, and *P. multiseries*. About 1000 each of small- and large-sized cells from randomly selected samples were measured. *Pseudo-nitzschia* spp. biovolume was estimated using a diamond-shaped box geometry:

$$V = \frac{L \times W^2}{2} \quad (1)$$

where V is volume (μm^3), L is the maximum length of the cell, and W is the maximum transapical width. The average cellular carbon was estimated as 11 and 104 pg C cell^{-1} for small and large cells, respectively (Olson et al. 2008).

Domoic acid—Discrete samples were collected throughout the grid survey at 1-, 5-, and 10-m depths. Particulate DA (pDA) was measured by filtering 1 L of seawater onto a 47-mm diameter nitrocellulose filter (HAWP04700 Millipore MF™-Membrane filters; 0.45-μm pore size) and freezing until analysis using a DA receptor binding assay method (Baugh et al. 2004) using a certified DA standard (DACS-1B, National Research Council, Canada). The limit of detection of the assay was 0.1 nmol L^{-1}, and the assay precision was approximately 5% CV. Positive identification of pDA in seawater samples collected from the Washington State coast has been previously confirmed by both high-performance liquid chromatography and liquid chromatography/tandem mass spectroscopy (Adams et al. 2000). Depth-integrated pDA was determined by trapezoidal integration for the upper 1–10 m of the water column by summing the areas of two four-sided polygons as follows:

$$pDA_{depth\,\mathrm{int.}} = \left[\frac{(b_1 + b_2) \times h}{2}\right] + \left[\frac{(b_2 + b_3) \times h}{2}\right] \quad (2)$$

where b_1, b_2, and b_3 are pDA concentrations at 1-, 5-, and 10-m depths, respectively, and h is the depth interval between sampling depths.

Nutrients—Water samples for dissolved inorganic nutrient analyses were collected at multiple depths to 500 m at the two inshore stations of each transect line and then at every other station continuing offshore. Unfiltered samples were collected in precleaned polypropylene tubes and analyzed for nitrate plus nitrite ($NO_3^- + NO_2^-$, hereafter referred to as nitrate), orthophosphate (PO_4^{3-}), and silicic acid ($Si[OH]_4$) with a Lachat QuikChem 8000 Flow Injection Analysis system (Lachat Instruments) using standard colorimetric techniques (Smith and Bogren 2001; Knepel and Bogren 2002; and Wolters 2002, respectively).

Chlorophyll determination—At each station, surface samples were analyzed for phytoplankton biomass as Chl *a* using either the acidification (2003 cruises; Parsons et al. 1984) or nonacidification (2004–2006 cruises; Welschmeyer 1994) in vitro fluorometric analyses after filtration onto Whatman GF/F filters (0.7-μm nominal pore size). Samples were extracted at sea in 90% acetone for approximately 24 h at -20°C, and the fluorescence was subsequently measured with a Turner Designs 10AU fluorometer calibrated at the beginning of each cruise with pure Chl *a*.

Satellite imagery—Sea-viewing wide-field-of-view sensor (SeaWiFS) imagery was acquired from the National Oceanic and Atmospheric Administration's Coastwatch Program. The images were processed with the latest version of SeaWiFS data analysis system (SeaDAS) 4.0, which uses an atmospheric correction that compensates for near-infrared water leaving radiance and absorbing aerosols (Stumpf et al. 2003). The resulting chlorophyll imagery was developed using the global OC4 algorithm, with 1-km resolution (O'Reilly et al. 2000).

Winds—Wind velocity vectors were constructed using wind speed and direction measurements obtained from observations at the Cape Elizabeth meteorological buoy (#46041, 47.34°N, 124.75°W; *see* Fig. 1a) maintained by the National Data Buoy Center. When these data were unavailable (01 May–21 June 2006), linear regressions with the nearby Destruction Island station (#DESW1, 47.68°N, 124.49°W; *see* Fig. 1a) were used to complete the time series.

Statistical relationships—Correlation analyses were conducted to determine relationships between ambient concentrations of pDA and *Pseudo-nitzschia* abundance and the physical–chemical–biological environmental properties observed during all cruises. To allow better comparability among cruises, only surface (1-m depth) data were included. Subsurface data were generally highly correlated

with those at the surface. Relationships determined for pDA used data only from sites where *Pseudo-nitzschia* were detected. The distributions of pDA concentrations and *Pseudo-nitzschia* abundances could not be transformed to meet the assumption of normality. Therefore, relationships were determined using the nonparametric Spearman's rank correlation analyses. The Spearman's rank difference correlation coefficient (r_s) indicates the strength of general monotonic relationships by measuring the association between ranks of variables. Relationships were determined over the survey grid and also within the eddy region and the nearshore zone (*see* definitions illustrated in Fig. 1a). All statistical analyses were conducted using the software package SPSS 14.0 (SPSS).

Results

In order to set the context for interpreting cruise data, a brief overview of the physical oceanography of the region is provided prior to detailed descriptions of survey grids, vertical profiles, time-series analyses, and statistical relationships between *Pseudo-nitzschia* and pDA with the physical, biological, and chemical properties.

Physical oceanography and nutrient supply: an overview—In general, coastal currents are southward along the outer shelf and slope in this region for most of the late spring to fall upwelling period (Hickey 1989). The shelf break jet, which flows southeastward along the British Columbia outer shelf, forms the outer limb of the Juan de Fuca eddy. This jet turns southeast as it passes the eddy and eventually is directed almost due south as it transits the Washington shelf and slope (MacFadyen et al. 2005). In general, once surface waters (and their resident phytoplankton and dissolved nutrients) escape from the Juan de Fuca eddy, they transit the Washington coast from north to south in ~10–20 d, depending on the current speeds at that time. Escape from the eddy generally occurs only during upwelling-favorable winds (MacFadyen et al. 2008). Inner shelf currents also are generally southward in the summer season but reverse quickly to northward during summer storms because of the downwelling-favorable wind stress. Currents in the surface frictional layer tend to move onshore or offshore relative to the direction of the mean current in response to downwelling- or upwelling-favorable winds, respectively. Onshore movement of water masses a distance of 20–40 km during a single storm is not atypical (MacFadyen et al. 2005). In addition to the persistent southward advection of water masses along the Washington shelf described previously, during summer storms a buoyant plume (warmer and fresher than ambient coastal water) from the Columbia River can move rapidly northward along the coast to at least La Push (LP, *see* Fig. 1; Hickey et al. 2005). Such a plume was visible on all but one (September 2005) of our ECOHAB-PNW cruises (not shown).

Phytoplankton blooms occur frequently in the eddy region (Trainer et al. 2002; MacFadyen et al. 2008) because of the persistent but variable nutrient supply, governed by estuarine dynamics, which include a mean outflow from the Strait of Juan de Fuca (Mackas et al. 1980; MacFadyen et al. 2008). In contrast, nutrient supply in the coastal upwelling area to the south is governed strongly by wind to the extent that macronutrient input to surface layers essentially ceases during downwelling-favorable conditions. Elevated nutrient concentrations in the eddy region also extend much further offshore compared to the coastal upwelling zone as the presence of the eddy leads to enhanced cross-shelf export of nutrient-rich Juan de Fuca water (MacFadyen et al. 2008).

Large-scale survey grid environmental conditions—The sampling grid (Fig. 1b) was surveyed under a variety of wind conditions (upwelling vs. downwelling) over 4 yr (Fig. 2). Although described in greater detail by MacFadyen et al. (2008), in brief, the grid survey in June 2003 took place during a period of strong upwelling following a short period of downwelling (Fig. 2). High-salinity (Fig. 3), low-temperature (not shown) water was observed next to the coast due to upwelling. The brief storm in June 2003 initiated the development of a lower-salinity, warmer plume from the Columbia River extending northward past Grays Harbor (GH) immediately adjacent to the coast (*see* Fig. 1 for locations). The July 2005 grid was sampled under strong upwelling-favorable winds. Although the spring transition was "delayed" in 2005 (Hickey et al. 2006), strong upwelling began on about 13 July before the full grid sampling, and colder, saltier water was observed along the coast except in the southern portion of the grid (Fig. 3). In spite of the strong upwelling, as in June 2003, Columbia River plume water was apparent on the two southern transect lines (at GH1, GH2, and KB2). This plume was likely a result of the storm of 07–12 July (Fig. 2).

Late summer grid surveys spanned a range of conditions varying from strongly upwelling-favorable winds (2003) to a moderately downwelling-favorable summer storm (2004), weak winds following sustained upwelling (2005), and, finally, a strong fall storm following an upwelling-favorable period (2006) (Fig. 2). Thus, in the fall of 2003, relatively saltier, colder water was observed along the Washington coast and extending well offshore of the Strait of Juan de Fuca (Fig. 3). Fresher, warmer water was observed along the Washington coast in late summer 2004, relative to 2003, consistent with the downwelling-favorable winds during the grid survey. A remnant Columbia River plume, slightly displaced offshore, was evident at southern stations (Fig. 3). In the September 2005 grid survey, although winds were weak and variable, colder, saltier water produced by the strong upwelling that preceded the survey was evident in the nearshore zone. The Juan de Fuca eddy was a distinct feature in both temperature (not shown) and salinity (Fig. 3). Fresher water from the Strait of Juan de Fuca wrapped around the eddy on its northern side. Nearshore water along the southern transect line was significantly warmer than at other stations, although the elevated salinity shows this was not the result of the Columbia River plume observed in some other cruises. Strong downwelling-favorable winds (Fig. 2) occurred during much of the grid survey of September 2006. However, upwelling-favorable winds had been so persistent and strong prior to the cruise (over a month) that cold,

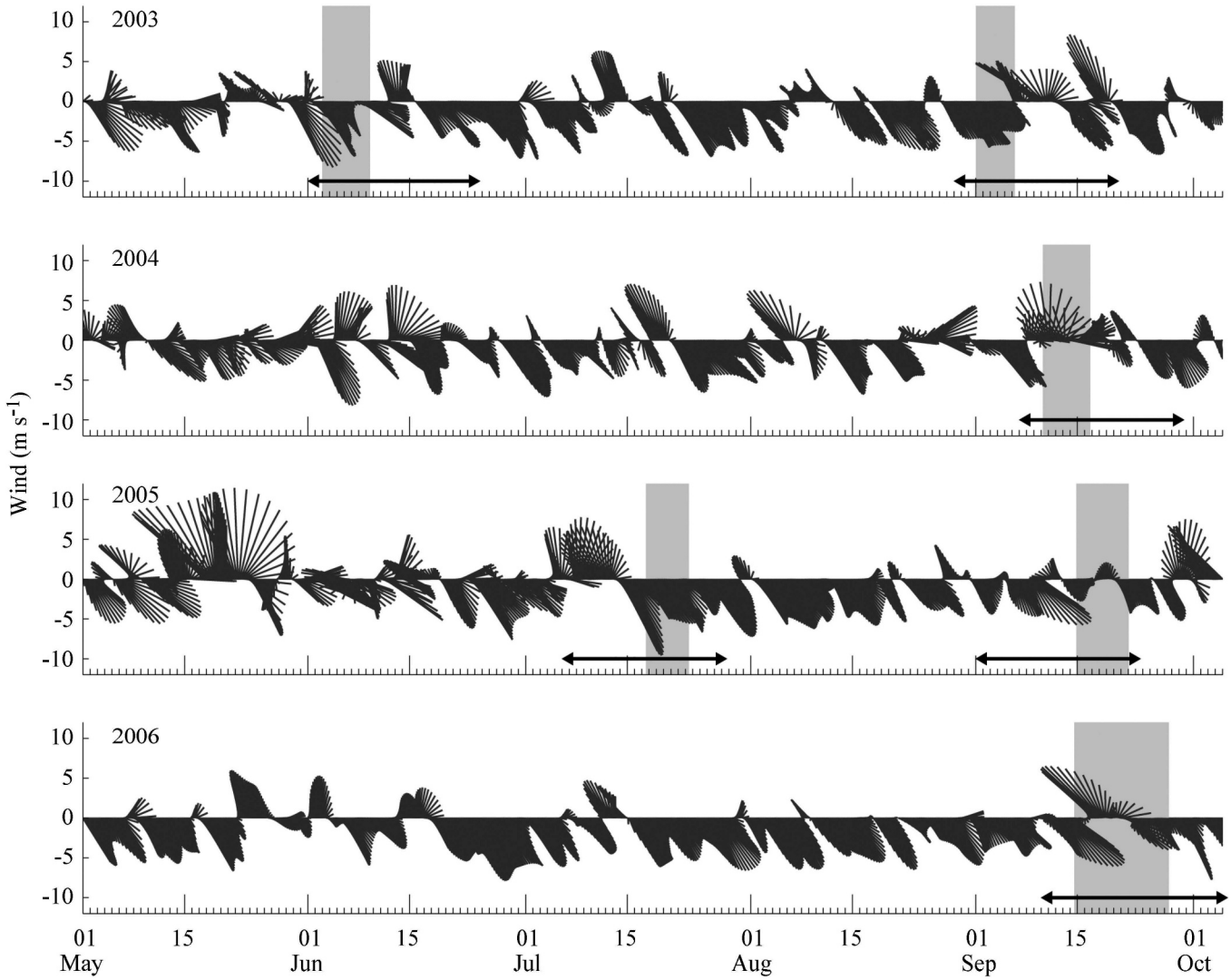

Fig. 2. Wind vectors for the May–October period during 2003–2006 measured at the Cape Elizabeth National Data Buoy Center buoy (location shown in Fig. 1). Wind vectors above the "0" line denote downwelling-favorable conditions, whereas those below denote upwelling-favorable conditions. The timing of the ECOHAB-PNW grid surveys and the 21-d cruises are shown as shaded areas and arrowed lines, respectively.

salty water was still observed over the entire coastal measurement region (salinity in Fig. 3). Surface nutrients were high over much of the grid (>10 μmol L^{-1} NO_3^-; not shown), and chlorophyll was unusually low in September 2006 (Fig. 4) over much of the Washington and Vancouver shelves.

Spatial variability of Pseudo-nitzschia *and pDA*—In this section, measurements of *Pseudo-nitzschia* and pDA are used to delineate spatial patterns and to determine whether relationships exist between their distributions. These data subsequently are expanded to include different depths (1, 5, and 10 m) to explore vertical variability in distributions. For simplicity, surface distributions of *Pseudo-nitzschia* are shown because the highest *Pseudo-nitzschia* abundance typically was found in surface (1 m) waters. The maximal *Pseudo-nitzschia* abundances were at 1 m (75% of the stations sampled) or 5 m (13% of the stations sampled); cell densities typically were lower in deeper waters. Maximum pDA concentrations occurred at the surface in 42% of the stations sampled and 31% at the 5-m depth; therefore, depth-integrated pDA is shown in Fig. 4b to emphasize "hot spots." There was no significant difference in the depth of maximal pDA concentration or *Pseudo-nitzschia* abundance between the early (June 2003 and July 2005) and late (September 2003, 2005, and 2006) season surveys.

Pseudo-nitzschia cells were observed in surface samples of the grid surveys at 36–96% of the stations (Table 1a; Fig. 4a). *Pseudo-nitzschia* sometimes were more abundant in the eddy region (September 2004 and July 2005) and sometimes more abundant in the nearshore zone (September 2005 and 2006; Fig. 4a) but were present in both the eddy and the nearshore zones during all cruises. There was a tendency for higher *Pseudo-nitzschia* concentrations to be associated with elevated Chl *a*, for example, on the edges of the eddy in June 2003, in the eddy region in September

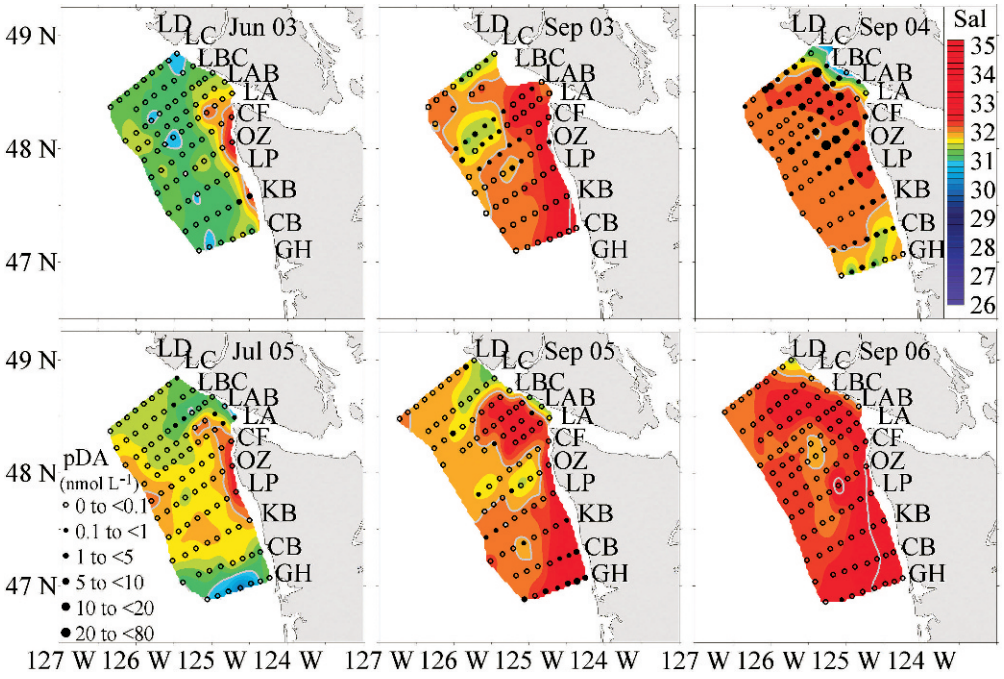

Fig. 3. Surface particulate DA concentrations (nmol L^{-1}) at each station during the grid survey are shown on surface salinity contours for the six cruises from June 2003 through September 2006. The limit of detection for pDA was 0.1 nmol L^{-1}.

2004, and along the southern Washington coast in September 2005. However, relatively high concentrations (>5000 cells L^{-1}) also were present in regions of low Chl *a*, such as near the northern Washington coast in September 2003 and at the stations furthest offshore in the eddy region in September 2006 (Fig. 4a).

Whereas *Pseudo-nitzschia* cells were observed at more than one-third of the surface stations sampled during each grid survey, pDA concentrations were detectable in only a fraction of these surface samples, with the exception of the September 2004 survey (Table 1a). During that survey, record-high *Pseudo-nitzschia* cell abundance (up to 13×10^6 cells L^{-1}) and pDA concentrations (up to 80 nmol L^{-1}) for this region were measured in the Juan de Fuca eddy and waters just south of it. This massive bloom event will be described in more detail elsewhere. During the September 2004 grid survey, 65% of the surface survey samples contained quantifiable pDA (Table 1a). The percentage of stations with quantifiable pDA at the surface was greater in the eddy region ($n = 61$) than in the nearshore stations ($n = 11$) during grid surveys in September 2003, September 2004, and July 2005 but not during the other cruises (Table 1a). Overall, no consistent relationship was observed between patterns of *Pseudo-nitzschia* abundance and those of pDA on any grid survey (Fig. 4).

The number of stations with detectable *Pseudo-nitzschia* cells was not significantly different when subsurface depths were added to the analysis of surface samples. For example, during the September cruises, the percentage of stations with detectable *Pseudo-nitzschia* increased by 0% (September 2003), 12% (September 2004), 2% (September 2005), and 5% (September 2006) when the deeper depths (5 and 10 m) were also included (Table 1b). In contrast, pDA was observed below 1-m depth but not at the surface at some stations during each cruise (compare Table 1a,b). During grid surveys on all cruises, 2–65% of the stations had detectable pDA in surface samples (Table 1a), and 3–78% of the stations had detectable pDA when all depths were considered (Table 1b). Similar to *Pseudo-nitzschia* cell numbers, the majority of quantifiable pDA was measured in surface samples.

An example of the variability in pDA concentrations with depth is shown in Figure 5, which shows pDA along a transect line through the eddy (LAB; *see* Fig. 1 for location), which was repeated twice during the June and September 2003 and July 2005 cruises. The extent of eddy development differed during each cruise, as evidenced from the variable upward bowing of deep salinity contours (Fig. 5). The greater upward penetration of deep, saline water observed in the late July and September surveys was consistent with the seasonal increase in the spatial extent of the eddy (Fig. 5; MacFadyen et al. 2008). In June 2003, pDA on the LAB transect line was observed at multiple depths to 50 m only on 21 June (survey 3). However, in September 2003, pDA concentrations were quantifiable at all depths to 20 m during both of the two surveys conducted. Low concentrations of pDA were measured on the LAB transect line during July 2005 at 15-m depth (08 July; survey 1) and 1–15-m depth (21 July; survey 2). In summary, low but quantifiable levels of pDA were measured as deep as 50 m (e.g., June 2003) in the region, but maximum concentrations were generally in the upper 20 m of the water column.

Temporal variability in Pseudo-nitzschia *abundance and pDA*—An assessment of the several-day variability in

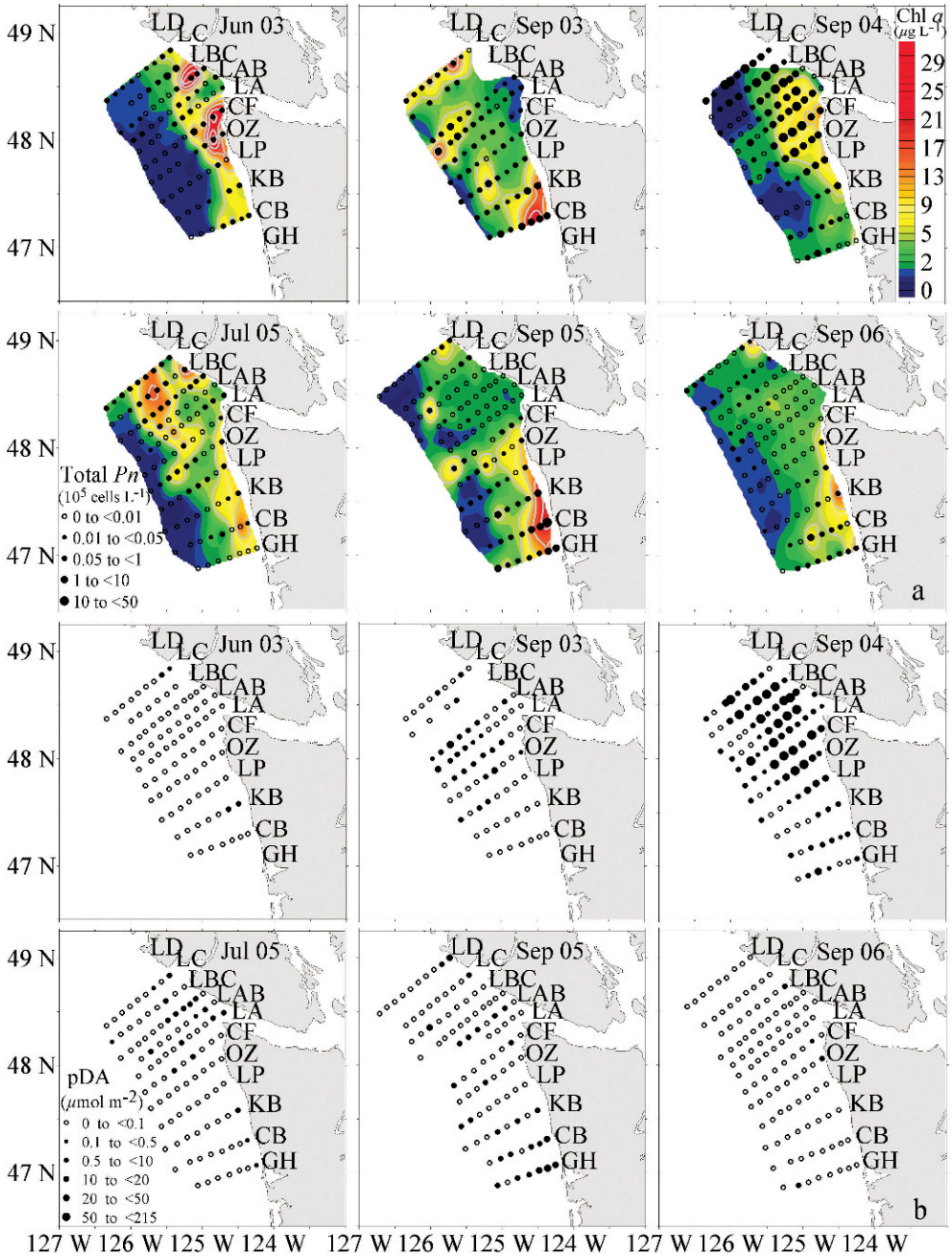

Fig. 4. (a) Surface abundances of total *Pseudo-nitzschia* (cells L^{-1}) shown on surface Chl *a* contours ($\mu g\ L^{-1}$) for June 2003 through September 2006 and (b) integrated pDA concentrations ($\mu mol\ m^{-2}$) for 1, 5, and 10 m during the grid survey for all six cruises. The limit of detection for pDA was 0.1 nmol L^{-1} and for *Pseudo-nitzschia* was 10^3 cells L^{-1}. Due to sample loss, cell abundances for stations CB05, CB07, GH04, GH05, GH06 were estimated from a linear regression of pDA vs. *Pseudo-nitzschia* concentrations from the filament region during the survey ($r^2=0.43$).

Pseudo-nitzschia abundance and pDA concentrations was obtained by comparing data from the 6–10-d period required to sample the grid (Table 1a, b) with all data from the entire 21-d cruises (Table 1c). Inspection of samples collected at 1-, 5-, and 10-m depths during the grid survey shows substantial differences in *Pseudo-nitzschia* abundance and pDA concentrations compared to the 21-d cruise period only in June 2003. In June 2003, pDA was not detected in surface waters during the grid survey (Fig. 6, survey 1) but was found in the eddy region during surveys 2 and 3 (*see* the following discussion), suggesting there was in situ production of DA within the eddy during the cruise.

Surveys conducted during the June 2003 cruise provided an estimate of the variability in *Pseudo-nitzschia* and depth-integrated pDA concentrations on time scales of several

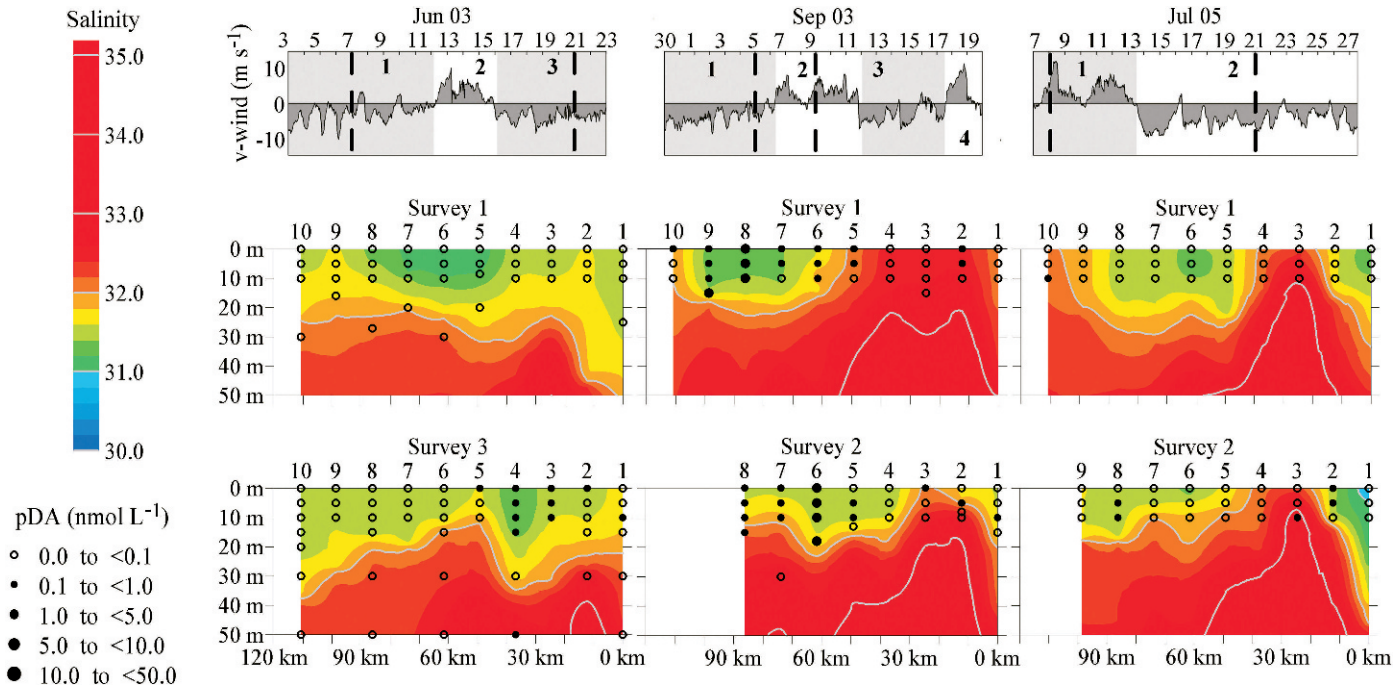

Fig. 5. Vertical transects of the LAB line (*see* Fig. 1 for location) showing particulate DA (nmol L^{-1}) on salinity contours to 50-m depth during three cruises, including surveys 1 and 3 (June 2003), surveys 1 and 2 (September 2003), and surveys 1 and 2 (July 2005). The limit of detection for pDA was 0.1 nmol L^{-1}. The wind data (*V* component) during each cruise with numbered survey periods indicating upwelling- or downwelling-favorable conditions are shown in upper panels. The dotted vertical lines illustrate the dates when the LAB transect line was sampled.

days (Fig. 6). *Pseudo-nitzschia* cells were observed at multiple stations during the grid survey, but measurable pDA concentrations were observed at only two of the southern nearshore stations (KB) and off Barkley Sound (LC; Fig. 6). Drifter trajectories coincident with this survey indicated predominantly southward flow, consistent with upwelling-favorable winds. The southern nearshore stations on the CB and KB transect lines (CB01, CB02, KB02) were influenced by the Columbia River plume at this time, which was generated during a storm that preceded the cruise (*see* Fig. 2). When winds shifted to downwelling-favorable after 12 June, three of the northern grid lines were resampled (survey 2). During this partial survey, higher concentrations of *Pseudo-nitzschia* were observed in the eddy region and were accompanied by low but measurable pDA at approximately half the stations sampled. Onshore water movement was consistent with drifter tracks during this period, suggesting that cells also moved onshore. Finally, when upwelling-favorable winds resumed on ~16 June, another partial survey (survey 3) was conducted. During this period, *Pseudo-nitzschia* cells were seen at most of the nearshore zone stations sampled and in the eddy region. Drifters again moved southward, consistent with the return of southward winds. Particulate DA concentrations were quantifiable at about 50% of the stations sampled, including several stations in the nearshore zone. Salinity data suggest that these latter stations were situated in the northern extension of the Columbia River plume, which was directed northward during the subsequent storm (Fig. 6).

The time series of vertical cross sections of pDA along the LAB transect line across the eddy during three cruises further illustrates temporal variability over periods of a week or less (Fig. 5). During the grid survey in June 2003, no measurable pDA was found along the LAB transect line. However, when the transect line was repeated on 21 June (survey 3), following the storm of 12–16 June, significant pDA was observed (Fig. 6). Surface salinity patterns (Fig. 6) show that this region of "new" pDA occurred on the margins of the developing Juan de Fuca eddy (*see* cyclonic trajectory of drifter off Cape Flattery in survey 2), which in the early season is evident in surface water properties as relatively saline water spreading offshore of Cape Flattery (MacFadyen et al. 2008). Elevated pDA was associated with water with salinities between 31.0 and 31.5 at 30–40 km from shore. Although pDA was detectable during survey 1 only at the nearshore LC stations (within the northwestward-flowing VICC), we note that approximately 2 weeks occurred between surveys 1 and 3; therefore, advection from outside the study area cannot be ruled out completely. However, both near-surface current measurements (location in Fig. 1; not shown) and the diagnostic model results from MacFadyen et al. (2008) show weak and variable flow in this region until ~20 June. Combined, these results are suggestive of in situ production of DA rather than advection of toxic cells from outside the eddy region.

During the first survey in September 2003, pDA was apparent in the relatively low salinity offshore water that originated from the Strait of Juan de Fuca and wrapped around the northern and western edges of the eddy region

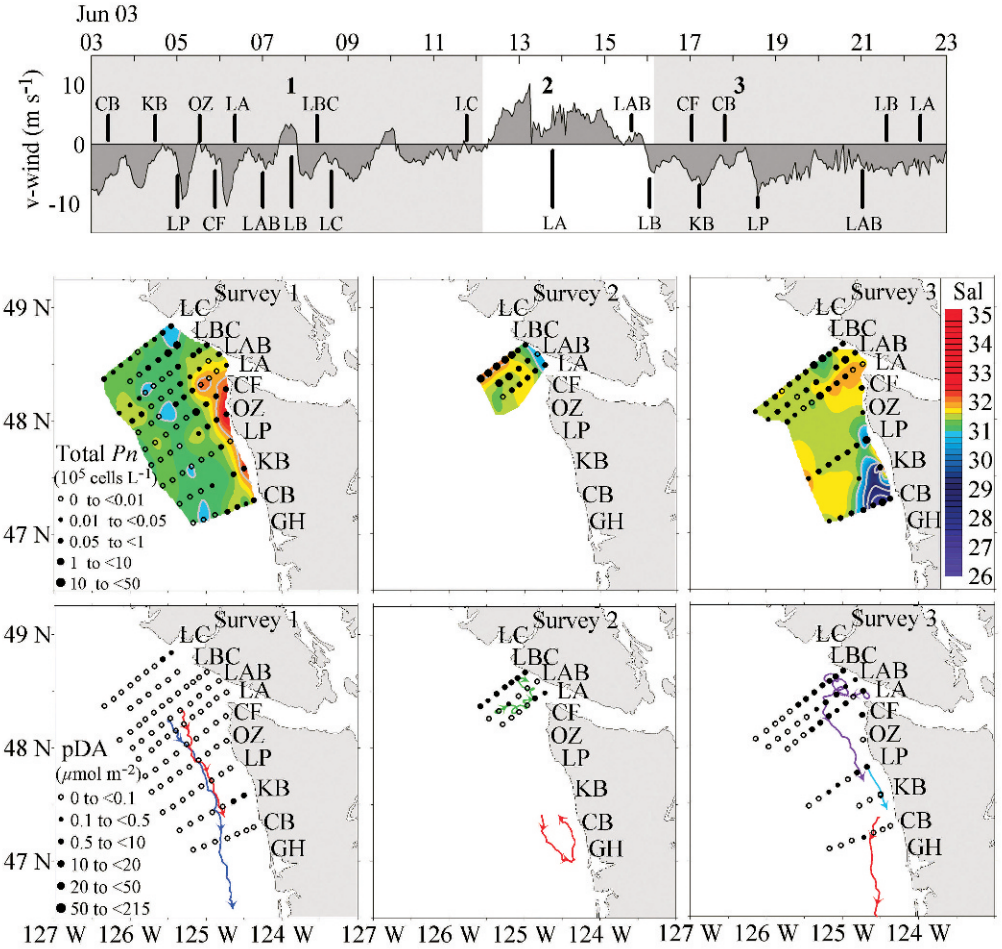

Fig. 6. Surface *Pseudo-nitzschia* abundance (cells L^{-1}, middle panels) and integrated pDA concentrations for 1, 5, and 10 m (μmol m^{-2}, lower panels) are shown during three survey periods of the June 2003 cruise. The limit of detection for pDA was 0.1 nmol L^{-1} and for *Pseudo-nitzschia* was 10^3 cells L^{-1}. Upper panel: Wind vectors (*V* component) during each of the three surveys are shown in shaded boxes. Line labels are shown on wind vectors to indicate timing of transect line sampling. Portions of drifter tracks corresponding to each survey are shown in lower panels. Color is used to distinguish the different drifters, and arrows signify drifter direction.

(Fig. 5; also *see* surface map, Fig. 3). When the transect was repeated several days later, the region of highest toxicity appears to have moved shoreward following the downwelling-favorable wind event (Fig. 2). In July 2005, toxin was observed at only one offshore station when the line was first sampled on 08 July (survey 1), following an extended period of upwelling winds and less than a day of downwelling winds (Fig. 5; also *see* wind setting prior to the cruise in Fig. 2). As part of the grid survey (*see* depth-integrated pDA in Fig. 4b), the transect was resampled on 21 July (survey 2), and toxin was found on both the western and the eastern edges of the eddy. In the interval between the two surveys, 4 d of downwelling winds were followed by 8 d of upwelling winds. Thus, for the July 2005 example, it is difficult to delineate how much of the pDA appeared to be due to in situ production within the eddy region relative to advective transport of toxin-bearing cells into the eddy region.

Relationship between eddy region and filament zone—Although remote sensing cannot provide insight to toxic vs. nontoxic conditions, satellite-derived estimates of Chl *a* on 02 September 2003 showed a surface tendril coincident with the strong southwestward flow over the shelf margins (MacFadyen et al. 2008) that was consistent with shipboard Chl *a* data (Figs. 1, 4a). This filament contained toxic cells and in the satellite image tended to the southeast toward the coast and intersected a high Chl *a* region on the central Washington shelf (Fig. 1a). Using drifter data and model results, MacFadyen et al. (2008) were able to demonstrate that water masses can escape from the eddy during such upwelling-favorable wind conditions. Indeed, upwelling was occurring during the September 2003 survey period and on the date of the satellite image (02 September; Fig. 2). The zone of highest Chl *a* in the nearshore region contained *Pseudo-nitzschia* (Fig. 4a) but no measurable surface pDA (Fig. 3). Combined, these data indicate that the toxic cells in the filament originated in the eddy and not from the nearshore zone.

Pseudo-nitzschia *species assemblages and pDA in the eddy vs. nearshore zone*—Species that were observed during

the six cruises included *P. fraudulenta*, *P. pungens*, *P.* cf. *pseudodelicatissima*, *P. cuspidata*, *P. delicatissima*, *P. australis*, *P. heimii*, *P. lineola*, *P. seriata*, and *P. multiseries* (Table 2). At times when the small *Pseudo-nitzschia* cells (the p/d/c group) were dominant, their abundance could reach numbers over several hundred thousand per liter. In general, the small *Pseudo-nitzschia* cells formed the largest blooms, with exceptions occurring during the September 2003 cruise when *P. heimiilfraudulenta* (Sta. CB01) and *P. australis* (Sta. LA11) numbered approximately 3.0×10^5 cells L^{-1} (Table 2). When cell numbers were 5.0×10^4 L^{-1} or less, larger cells, such as *P. heimii*, *P. australis*, *P. fraudulenta*, *P. seriata*, and *P. multiseries*, could also dominate the *Pseudo-nitzschia* assemblage.

The highest levels of pDA (>5 nmol L^{-1}) were measured at sites with both low (4.9×10^4 cells L^{-1} on 13 September 2003 at KB05) and high (3.3×10^6 cells L^{-1} on 15 September 2004 at LBC02) *Pseudo-nitzschia* concentrations (Table 2). The reverse also was true; for example, in September 2006, although *Pseudo-nitzschia* cells numbered 3.9×10^5 cells L^{-1} at Sta. CB05 in the filament zone, pDA was below the level of quantification (Table 2). Very low concentrations of pDA also were observed during the July 2005 and September 2006 cruises in spite of the presence of $>5.0 \times 10^4$ *Pseudo-nitzschia* cells L^{-1}. During the September 2004 cruise, when the highest values of pDA were observed, the *P. cuspidata* cell numbers often exceeded 10^6 cells L^{-1} and the relative toxin levels observed at eddy stations were approximately proportional to the cell numbers. Nearshore pDA and *Pseudo-nitzschia* abundances were much lower than levels observed in the eddy on that cruise (Table 2). In September 2005, the stations with moderate pDA concentrations (>1 nmol L^{-1}) had cell densities that varied by almost two orders of magnitude (3.6×10^4 to over 1×10^6 cells L^{-1} of the small *Pseudo-nitzschia* size group [p/d/c]), both in the eddy and in the nearshore zone.

Species information may help us determine whether toxic blooms developed in situ within the nearshore zone or were transported from the eddy region. While little can be discerned if both nearshore and eddy region waters contain a similar *Pseudo-nitzschia* species, a difference in species composition in samples measured only a few days apart would suggest that independent processes were responsible for the adjacent blooms. Indeed, species composition differed significantly between the eddy and nearshore regions on two occasions. The first was in September 2003, when *P. australis* dominated in the eddy region, whereas *P. heimiilfraudulenta* (these two species could not be distinguished by SEM) dominated in the nearshore zone (CB01 on 01 September 2003; Table 2). The difference in *Pseudo-nitzschia* species composition suggests that the non–toxin-bearing *Pseudo-nitzschia* in the nearshore zone did not originate from the eddy. The dominant phytoplankton group near the coast (diatom, 91%) was different from that in the filament (dinoflagellate, up to 47%; Table 3), again consistent with the suggestion that nearshore and eddy or filament phytoplankton had different origins. A sample from the filament 1 week later (KB05 on 13 September 2003) compared to the eddy samples at LA11 on 04 September 2003 and LA08 on 08 September 2003 (Table 2) indicated similar compositions of *Pseudo-nitzschia* species in the eddy and filament (*P. australis* was dominant).

The second case where species composition differed in the eddy and in the nearshore zone was during the July 2005 cruise, when toxigenic *Pseudo-nitzschia* in the eddy region were dominated by the *P. multiseries* group, whereas the non–toxin-bearing cells near the coast were dominated by *P. delicatissima* and *P. pungens* (LP01; Table 2). In addition, the diatom community composition was very different in the nearshore zone and eddy or filament stations selected for analysis (Table 3).

Pseudo-nitzschia *as part of the total phytoplankton community*—Although *Pseudo-nitzschia* spp. reached extremely high abundances at times (>10^6 cells L^{-1}; Tables 2, 3), they almost always represented a small component of the total phytoplankton carbon biomass (generally <7%; Table 3). Only in two instances was their biomass contribution more substantial, and even then it represented well under a quarter of the phytoplankton biomass (approximately 12 and 17% at a nearshore [September 2003] and an eddy [September 2004] station, respectively; Table 3) regardless of whether diatoms dominated the assemblage or not. Diatom blooms occurred in the eddy, filament, and nearshore regions, but the dominant diatom taxa were quite variable (Table 3). In the eddy region, however, there were several nondiatom blooms, most notably dinoflagellates (*Ceratium* and *Prorocentrum* spp.) in September 2003 and a euglenoid (*Eutreptiella* sp.) in September 2004. *Pseudo-nitzschia* was the dominant diatom taxa only during the September 2004 euglenoid bloom in the eddy and in a *Ceratium*-dominated community in what appeared to be an aged eddy filament (Sta. CB07) in September 2003. Diatoms dominated all observed nearshore blooms with the exception of a *Cochlodinium polykrikoides* bloom in September 2006 at the inner stations of the southernmost transect line on a repeat survey (not shown), which were at the margin of the northern extent of the Columbia River plume.

Statistical relationships of Pseudo-nitzschia *and pDA with environmental variables*—Spearman's rank correlation coefficients and associated significance values for relationships of *Pseudo-nitzschia* and pDA with the physical–chemical–biological variables are given in Table 4. A weak but significant positive relationship was found between *Pseudo-nitzschia* and pDA ($r_s = 0.55^{**}$, $n = 323$), reflecting the finding that *Pseudo-nitzschia* detected during cruises were not always producing toxin. Chl *a* concentrations were weakly but significantly correlated with *Pseudo-nitzschia* abundances ($r_s = 0.52^{**}$, $n = 531$). This relationship was stronger when only the September 2004 grid survey, during which record *Pseudo-nitzschia* abundances were detected for this region, was considered ($r_s = 0.72^{**}$, $n = 83$; Fig. 7). No significant correlation existed for pDA and *Pseudo-nitzschia* with temperature, and only a weak positive relationship existed with salinity (Table 4). The only significant positive correlations between pDA and nutrients over the entire sampling grid were observed with

Table 2. *Pseudo-nitzschia* species and toxicity observed in selected surface samples collected in the eddy, its filaments (in bold), and nearshore zone during surveys conducted from 2003–2006 in the Pacific Northwest study region.

Eddy						Nearshore zone or filament				
Cruise	Date	Sta.	*Pn* (cells L^{-1})	*Pn* species (%)*	pDA (nmol L^{-1})	Date	Sta.	*Pn* (cells L^{-1})	*Pn* species (%)*	pDA (nmol L^{-1})
1	14 Jun 03	LA02	8000	pun(60), p/d/c(20), aus(17), multi(3); *n*=121	0.33	04 Jun 03	KB02	21,000	heimii(75), pun(13), aus(4), fraud(4), p/d/c(4); *n*=53	1.26
1	15 Jun 03	LAB02	5000	pun(58), aus(26), multi(10), p/d/c(5); *n*=165	0.05	04 Jun 03	KB01	24,000	pun(70), heimii(18), p/d/c(12); *n*=59	1.48
2	04 Sep 03	LA11	278,000	aus(97), p/d/c(2), heimii(1); *n*=342	2.54	01 Sep 03	CB01	324,000	heimii/fraud(96), p/d/c(3), aus(1); *n*=290	0
2	08 Sep 03	LA08	69,000	aus(84), deli(13), heimii(7), pun(1); *n*=131	0.41	**13 Sep 03**	**KB05**	**49,000**	**aus(98), multi(1), pun(1); *n*=264**	**9.7**
3	13 Sep 04	CF04	1,467,000	cusp(96)†, fraud(2), pun(1), aus(1); *n*=344	12.65	**10 Sep 04**	**CB03**	**67,000**	**cusp(98), fraud(2); *n*=298**	**1.02**
3	14 Sep 04	LAB03	1,900,000	cusp(99), aus, fraud; *n*=402	16.42	11 Sep 04	KB01	250,000	cusp(99), fraud(1), multi; *n*=269	0.21
3	15 Sep 04	LBC02	3,280,000	cusp(98), deli(1), pun(1); *n*=177	20.25	**23 Sep 04**	**KB03**	**2,340,000**	**cusp(99), fraud(1); *n*=180**	**77.65**
3	15 Sep 04	LB06	1,040,000	cusp(99), multi, aus, fraud; *n*=233	7.65	**27 Sep 04**	**KB05**	**28,000**	**cusp(96), heimii(3), pun(1); *n*=77**	**1.60**
4	22 Jul 05	LB03	5333	multi(47), aus/fraud(27), p/d/c(11), pun(1); *n*=73	0.09	19 Jul 05	LP01	12,000	deli(58), pun(24), heimii(12), fraud(6); *n*=17	0
4	22 Jul 05	LB08	53,077	multi(32), seriata (34), p/d/c(16), pun(12), fraud(6); *n*=82	0.19	**19 Jul 05**	**LP04**	**53,077**	**fraud(50), pun(28), multi(6), deli(6), heimii(6), psdeli(3), seriata(1); *n*=72**	**0**
5	19 Sep 05	LAB06	1429	p/d/c(36), pun(34), heimii(28), multi(2); *n*=61	0.19	14 Sep 05	GH01	299,231	p/d/c(99), heimii(1); *n*=300	1.08
5	20 Sep 05	LBC07	36,000	p/d/c(98), heimii(2); *n*=212	2.21	15 Sep 05	CB01	1,126,923	p/d/c(92), heimii(7), fraud(1); *n*=132	1.21
5						**15 Sep 05**	**GH03**	**43,846**	**p/d/c(90), heimii(10); *n*=78**	**1.17**
6	26 Sep 06	LD08	80,714	p/d/c(68), heimii(30), multi(1), lineola; *n*=79	0	**14 Sep 06**	**GH05**	**73,846**	**p/d/c(49), heimii(43), fraud(5), multi(3); *n*=139**	**0.04**
6	27 Sep 06	LE06	50,769	p/d/c(65), heimii(35), lineola; *n*=47	0	14 Sep 06	GH01	14,600	fraud(68), pun(23), p/d/c(6), aus(1); *n*=98	0
6						**15 Sep 06**	**CB05**	**388,462**	**p/d/c(83), heimii(15), fraud(3), pun(1); *n*=238**	**0**
6						16 Sep 06	LP01	9230	seriata(33), heimii(31), pun(16), multi(13), fraud(4), p/d/c(3); *n*=55	0

* fraud, *P. fraudulenta*; pun, *P. pungens*; aus, *P. australis*; multi, *P. multiseries*; cusp, *P. cuspidata*; heimii, *P. heimii*; deli, *P. delicatissima*; lineola, *P. lineola*; seriata, *P. seriata*. The p/d/c notation is used to describe the *P. pseudodelicatissima/delicatissima/cuspidata* complex. These species often were indistinguishable by SEM, and TEM could not be performed on all samples. Percentage of a species in each sample is shown in parentheses. When no percentage is noted, the species is present at less than 1%. *n*=the number of cells identified by SEM to determine the % of each species in a sample.

† *P. cuspidata* was identified by TEM and SEM in samples collected during the September 2004 cruise. This is a new species resulting from the recent separation of *P. pseudodelicatissima* into three species (Lundholm et al. 2003). Therefore, *P. cuspidata* is not positively identified in samples prior to 2004; however, the abbreviation p/d/c is used to describe the small *Pseudo-nitzschia* species complex.

Table 3. The contribution of *Pseudo-nitzschia* biomass to total phytoplankton biomass (as carbon) and dominant phytoplankton taxa groups from selected samples from the eddy and nearshore regions of the Pacific Northwest study region. Percentage of each group in a sample is shown in parentheses.

Cruise	Date (GMT)	Sta.	Location	*Pseudo-nitzschia* (cells L^{-1})	*Pseudo-nitzschia* biomass (μg C L^{-1})	Total biomass (μg C L^{-1})	*Pn* (% of biomass)	Total Chl *a* (μg L^{-1})	Dominant phytoplankton group	Dominant diatom groups*
1	04 Jun 03	KB01	Nearshore	6.3×10^4	1.67	79.49	2.10	8.59	Diatom (91)	*Chaet* (43), *Thal* (25)
1	15 Jun 03	LAB05	Eddy	5.63×10^4	1.01	214.79	0.47	18.26	Diatom (96)	*Thal* (40), *Chaet* (30)
2	01 Sep 03	CB01	Nearshore	1.32×10^5	11.36	94.47	12.02	8.30	Diatom (91)	*Thal* (58)
2	06 Sep 03	LA10	Eddy	9.40×10^4	2.71	171.35	1.58	16.27	Dinoflagellate† (47)	*Thal* (54), *Cosc* (27)
2	09 Sep 03	LB07	Eddy	5.30×10^4	1.14	109.52	1.04	5.03	Dinoflagellate† (40)	*Cosc* (71)
2	14 Sep 03	CB07	Filament	2.30×10^4	2.02	52.30	3.86	1.00	Dinoflagellate† (40)	*Pn* (83)
3	12 Sep 04	CF04	Eddy	3.99×10^6	52.15	307.43	16.96	10.70	Euglenoid (51)	*Pn* (63)
3	14 Sep 04	LB05	Eddy	6.16×10^5	6.78	160.03	4.23	2.77	Euglenoid (48)	*Pn* (33), *Thal* (29)
3	15 Sep 04	LBC05	Eddy	5.07×10^5	6.32	166.19	3.80	2.03	Euglenoid (54)	*Pn* (61), *Thal* (24)
4	09 Jul 05	GH03	Filament	3.08×10^3	0.25	33.73	0.75	0.78	Diatom (40)	*Chaet* (32), *Guin* (23)
4	18 Jul 05	CB02	Nearshore	2.20×10^4	1.03	460.38	0.22	17.59	Diatom (85)	*Thal* (21), *Ent* (20) *Trop* (16), *Pleur* (14)
4	22 Jul 05	LB01	Eddy	9.3×10^4	2.42	212.21	1.14	8.83	Diatom (89)	*Chaet* (47)
4	22 Jul 05	LB05	Eddy	3.41×10^4	3.55	106.86	3.32	8.28	Diatom (79)	*Chaet* (47), *Thal* (35)
5	14 Sep 05	GH01	Nearshore	1.10×10^6	12.79	357.17	3.58	11.69	Diatom (86)	*Lept* (88)
5	15 Sep 05	CB02	Nearshore	6.02×10^5	11.46	702.09	1.63	13.89	Diatom (85)	*Lept* (74)
6	14 Sep 06	GH02	Nearshore	5.70×10^4	4.15	259.30	1.60	24.85	Diatom (89)	*Thal* (88)
6	15 Sep 06	CB02	Nearshore	4.26×10^4	3.68	53.52	6.88	6.55	Diatom (62)	*Thal* (61)
6	30 Sep 06	GH02	Nearshore	4.57×10^4	0.95	724.94	0.13	14.70	Dinoflagellate‡ (86)	*Lept* (22), *Thal* (17)

* *Chaet*, *Chaetoceros*; *Thal*, *Thalassiosira*; *Cosc*, *Coscinodiscus*; *Trop*, *Tropodoneis*; *Pn*, *Pseudo-nitzschia*; *Guin*, *Guinardia*; *Ent*, *Entomoneis*; *Pleur*, *Pleurosigma*.
† *Ceratium* and *Prorocentrum* spp.
‡ *Cochlodinium polykrikoides*.

nutrient ratios (r_s = 0.19* and 0.27* for N : P and Si : P, respectively; Fig. 8). When September 2004 data were removed from the analyses, only the correlation with N : P remained significant (r_s = 0.19*, n = 121). Finally, positive correlations were observed between nutrients, most nutrient ratios, and pDA in the eddy region, whereas these relationships were negative in the nearshore region (Table 4).

Table 4. Spearman's rank correlation coefficients (r_s) for particulate DA concentrations (pDA) and *Pseudo-nitzschia* spp. abundances with the physicochemical variables chlorophyll *a* (Chl *a*), temperature, salinity, nitrate ($NO_3^-+NO_2^-$), phosphate (PO_4^{3-}), silicic acid ($Si[OH]_4$), and the nutrient ratios nitrate : phosphate (N : P), nitrate : silicic acid (N : Si), and silicic acid : phosphate (Si : P). Analyses used surface observations from survey data for all cruises. For each entry of $r_{s,df}$, the subscript "df" indicates the number of observations used in the correlation. Significance at the 95% and 99% confidence levels (i.e., $p \le 0.05$ and 0.01) are indicated by * and **, respectively. Correlations with *Pseudo-nitzschia* abundances (in bold) were calculated using all available observations, whereas correlations with pDA concentrations were calculated using only observations from stations where *Pseudo-nitzschia* cells were detected.

	Whole grid		Eddy region	Nearshore region
	pDA	*Pseudo-nitzschia*	pDA	pDA
Pseudo-nitzschia	0.55_{323}**	**1.00**	0.59_{157}**	0.60_{48}**
pDA	1.00	$\mathbf{0.49_{564}}$**	1.00	1.00
Chl *a*	0.19_{307}**	$\mathbf{0.52_{531}}$**	0.20_{143}*	0.18_{48}
Temperature	$<0.01_{323}$	$\mathbf{-0.06_{579}}$	-0.16_{157}*	0.38_{48}**
Salinity	0.13_{323}*	$\mathbf{0.11_{579}}$*	0.21_{157}**	-0.13_{48}
$NO_3^-+NO_2^-$	0.08_{188}	$\mathbf{-0.08_{331}}$	0.25_{88}*	-0.37_{45}*
PO_4^{3-}	0.03_{165}	$\mathbf{-0.10_{286}}$	0.14_{72}	-0.35_{40}*
$Si(OH)_4$	0.09_{188}	$\mathbf{-0.03_{331}}$	0.26_{88}*	-0.48_{45}**
N : P	0.19_{163}*	$\mathbf{0.05_{283}}$	0.37_{70}**	-0.17_{40}
N : Si	0.10_{188}	$\mathbf{-0.08_{331}}$	0.25_{88}*	-0.25_{45}
Si : P	0.27_{162}**	$\mathbf{0.34_{282}}$**	0.42_{70}**	0.24_{39}

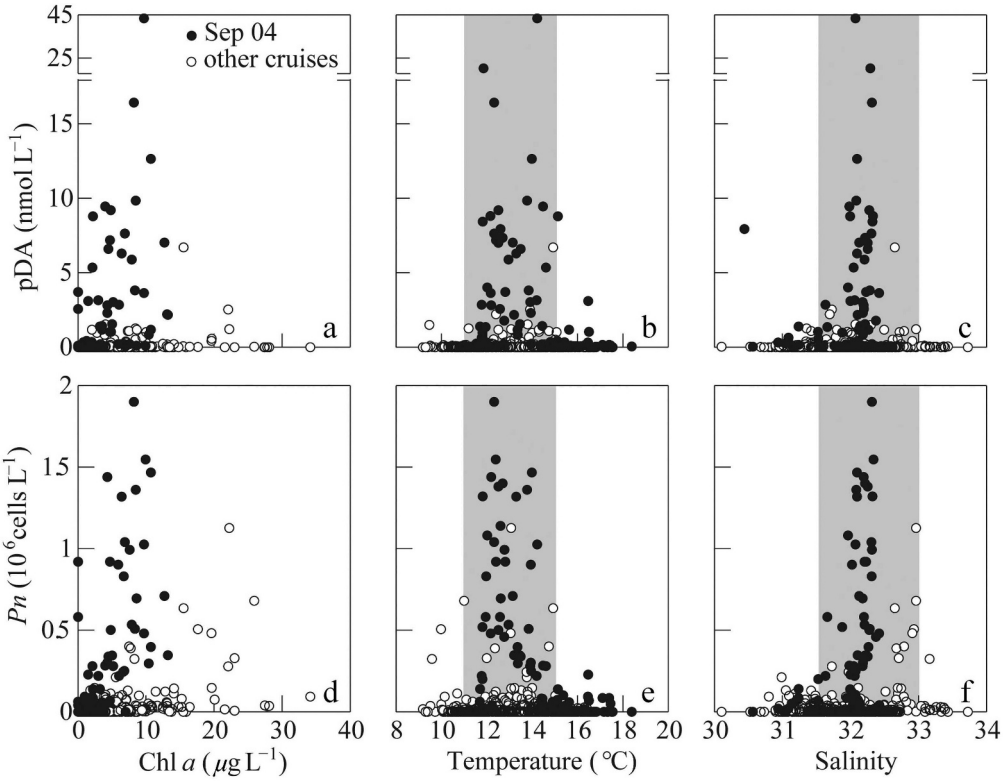

Fig. 7. (a–c) Particulate DA concentrations and (d–f) *Pseudo-nitzschia* spp. abundances (*Pseudo-nitzschia*) vs. Chl *a*, temperature, and salinity. Shaded regions indicate "windows" of temperature (11–15°C) and salinity (31.5–33.0) values where high abundances of *Pseudo-nitzschia* and pDA concentrations are observed. *Pn* = *Pseudo-nitzschia*.

Discussion

Spatial and temporal variability of Pseudo-nitzschia *and pDA in the Juan de Fuca eddy—Pseudo-nitzschia* cells were widespread off the Washington coast during all six cruises and were found in both the nearshore and eddy regions (Fig. 4a). However, these cells often were not producing detectable levels of pDA. Were the cells in the Juan de Fuca eddy region more likely to produce pDA than those in the nearshore upwelling zone? In the 21-d time scale of a cruise, some toxin always was measured in the eddy region (Table 1a,b). Over the course of the project, pDA was measured in ≥9% of the total samples collected at 1-, 5-, and 10-m depths within the eddy on all cruises except September 2006, when pDA occurred at only 1% of the eddy stations (Table 1c). In contrast, pDA was measured in <8% of the samples collected in the nearshore region on any cruise. In June 2003, rapid changes in levels of pDA in the eddy region were observed between the initial survey (*Pseudo-nitzschia* present but no pDA detected) and the following partial surveys (*Pseudo-nitzschia* and pDA present; Fig. 6). The upwelling period during the initial survey (survey 1) was followed by a storm during which *Pseudo-nitzschia* in the eddy produced toxin in situ and continued to produce pDA as winds shifted to upwelling-favorable again (Fig. 6). On several other cruises, pDA was observed on repeated survey lines over the 21-d cruise. These data support our initial hypothesis that the Juan de Fuca eddy is an initiation site for toxin-producing *Pseudo-nitzschia* and that although toxin levels were highly variable, pDA was measured in the eddy at some point over a 21-d time period (Table 1c).

Initiation sites for toxigenic blooms—One of the primary ECOHAB-PNW goals was to differentiate in situ development of toxic blooms in nearshore regions from advection of toxic blooms from other regions, such as the Juan de Fuca eddy. Our research suggests that toxic blooms do develop in the eddy and that such blooms may escape the eddy and move southward along the Washington coast (Fig. 1a; MacFadyen et al. 2008). It is less clear whether toxic blooms ever develop in actively upwelling coastal water, in downwelling water, or in Columbia River plume water, all of which can occur within 10–20 km of the coast. Two of the sampling sites where pDA was measured in the nearshore waters were located in close proximity to the northward-moving Columbia River plume rather than recently upwelled water, suggesting that these toxic cells were advected onshore either from offshore toxic cell populations or from farther south (plume water originates at the southern end of the Washington coast). In June 2003, the station nearest the coast (Sta. KB01) was in recently upwelled water; the adjacent station (Sta. KB02) was located in a mixture of upwelled and plume water (*see* salinity front in Fig. 6). Indeed, the dominant *Pseudo-nitzschia* species at Sta. KB02 was different than in the

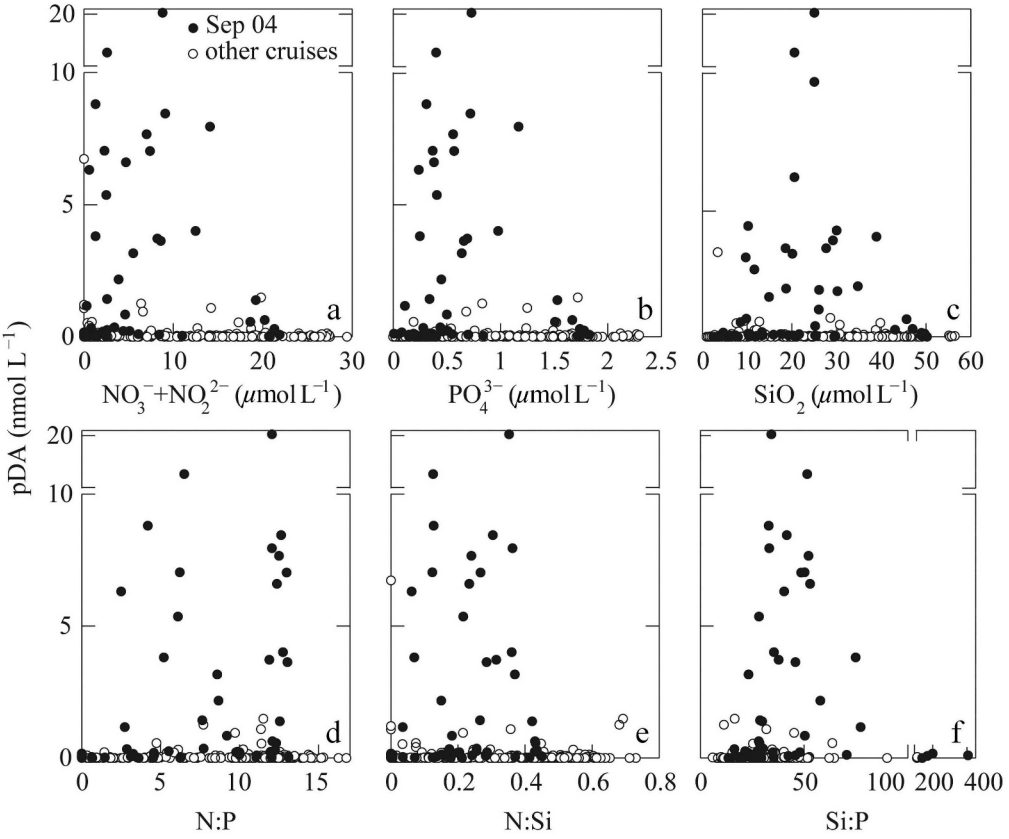

Fig. 8. Particulate DA concentrations vs. ambient concentrations of (a) nitrate ($NO_3^- + NO_2^-$), (b) orthophosphate (PO_4^{3-}), and (c) silicic acid ($Si[OH]_4$) and elemental ratios of (d) $NO_3^- : PO_4^{3-}$, (e) $NO_3^- : Si(OH)_4$, and (f) $Si(OH)_4 : PO_4^{3-}$.

eddy region, consistent with their origination from different sources (Table 2).

In September 2004, pDA was observed at most of the nearshore stations, and maximum pDA generally was observed offshore (Fig. 4b). These results are consistent with the onshore movement of toxic blooms during the downwelling wind events that occurred during this survey. Stations with detectable pDA along the southern transect lines again were within plume water or on the edges of the plume. Analysis of *Pseudo-nitzschia* species at selected stations (*see* the following discussion) indicated that species composition was very similar in the eddy region, in its filaments, and in the nearshore zone (Table 2), consistent with an advective source for the nearshore zone samples with pDA.

Surface waters in September 2005 were significantly warmer (not shown) along the southernmost transect line (GH) compared to other grid stations, and depth-integrated pDA concentrations were high along most of this line (Fig. 4b). *Pseudo-nitzschia* species at the southern stations were similar to those north of the GH transect line (Table 2; *see* Sta. GH01, CB01, and GH03 on 14–15 September 2005 compared with eddy stations at LAB06 and LBC07 on 19–20 September 2005), consistent with a northern source. The southward shelf break jet was stronger during this survey than in the other surveys (MacFadyen et al. 2008), supporting the view that toxic cells were being advected southward across this transect line. Data from ECOHAB-PNW moored arrays in the eddy (48°17.77N, 125°27.28W) and off Kalaloch (47°35.78N, 124°35.90W) confirm persistent southward flow from midshelf and over the slope over the 2 weeks before this survey. At 5-m depth, water moved 87 km southward from the edge of the eddy in 5 d and 176 km in 10 d prior to the measurements at station GH01 on 14 September 2005. Although in situ growth and toxin formation cannot be completely ruled out, it appears likely that the source of the water off the southern transect line of the grid was likely the same water mass originating from the eddy region 5–10 d prior to the station sampling. In summary, toxin at nearshore stations was rare unless associated with a recent storm (onshore transport, as in September 2004) or with the Columbia River plume.

Pseudo-nitzschia *species and related pDA concentrations in the Pacific Northwest*—The species of Pseudo-nitzschia that were positively identified by SEM and/or TEM during our cruises were *P. cuspidata*, *P.* cf. *pseudodelicatissima*, *P. delicatissima*, *P. pungens*, *P. heimii*, *P. fraudulenta*, *P. australis*, *P. lineola*, *P. seriata*, and *P. multiseries*. Based on a combination of laboratory studies with cultured isolates from these cruises (Baugh et al. 2006; Auro 2007), coastal monitoring studies through the Olympic Region Harmful Algal Bloom (ORHAB) program (Trainer and Suddleson

2005), and estimates of specific cellular toxicities in the field during these cruises (Baugh et al. 2006), we conclude that *P.* cf. *pseudodelicatissima*, *P. cuspidata*, *P. multiseries*, and *P. australis* pose the greatest threat to coastal fisheries. This conclusion stems from the probability that these smaller cells can form dense, toxic blooms or the large cells can form moderate blooms with high specific toxicities. For example, *P.* cf. *pseudodelicatissima* attained densities of 15 $\times$ 10^6 cells L^{-1} with maximum specific cellular toxicity of 0.3 pg DA $cell^{-1}$ (Adams et al. 2000), and *P. cuspidata* achieved densities of 13 $\times$ 10^6 cells L^{-1} with maximum specific cellular toxicity of 80 pg DA $cell^{-1}$ (September 2004 cruise average = 5 pg DA $cell^{-1}$, range 0.1–80 pg DA $cell^{-1}$, n = 55 [zeros excluded]), while *P. australis* has been estimated to contain up to 94 pg DA $cell^{-1}$ in samples from the Washington coast (Baugh et al. 2006). Although at times present in substantial numbers, *P. fraudulenta*, *P. pungens*, and *P. heimii* appear to pose little threat to fisheries because, in the absence of species known to produce high cellular DA, such as *P. australis*, little or no pDA was measured in samples containing these species (Table 2; *see* CB01 on 01 September 2003 and LP04 on 19 July 2005).

It is common for potentially toxic *Pseudo-nitzschia* cells, such as *P.* cf. *pseudodelicatissima* and *P. australis*, to be present without detectable concentrations of DA (Trainer et al. 2000), adding to the difficulty in predicting DA levels and specific cellular toxicities from the highly variable *Pseudo-nitzschia* species assemblages found off the Washington coast (Table 2). The species of *Pseudo-nitzschia* that are frequently observed have varying cellular toxicities ranging from 0 to almost 100 pg DA $cell^{-1}$ (Stehr et al. 2002; Baugh et al. 2006). Similar species assemblages of *Pseudo-nitzschia* found in similar abundance but at different locations (nearshore zone vs. eddy) can produce vastly different levels of DA (Trainer et al. 2002). For example, during September 2004, similar *Pseudo-nitzschia* species assemblages were seen at Sta. KB01 (nearshore) and Sta. CB03 (filament); however, the cells in the nearshore zone (2.5 $\times$ 10^5 cells L^{-1}) produced significantly less pDA (0.2 nmol L^{-1}) than the *Pseudo-nitzschia* cells in the filament (6.7 $\times$ 10^4 cells L^{-1}, 1.0 nmol L^{-1} pDA; Table 2). For September 2004, the average *Pseudo-nitzschia* number nearshore was 1.2 $\times$ 10^5 cells L^{-1} (range = 5.0 $\times$ 10^3–4.0 $\times$ 10^5 cells L^{-1}), average pDA nearshore was 1.1 nmol L^{-1} (range = 0.1–3.2 nmol L^{-1}, n = 19), average *Pseudo-nitzschia* number in the filament was 2.5 $\times$ 10^5 cells L^{-1} (range = 1.0 $\times$ 10^3–1.3 $\times$ 10^6 cells L^{-1}), average pDA in the filament was 4.0 nmol L^{-1} (range = 0.1–43.3 nmol L^{-1}, n = 68). This large variability in toxin production by *Pseudo-nitzschia* species prevents prediction of DA levels based on the abundance of *Pseudo-nitzschia* alone.

In the September 2004 cruise, *P. cuspidata* was observed as the single blooming *Pseudo-nitzschia* species (>95% of the *Pseudo-nitzschia* assemblage) in both the nearshore zone and offshore (Table 2). Small *Pseudo-nitzschia* species dominated in three out of four late season (i.e., early fall) cruises. Smaller species have a physical advantage over larger cells in waters with low or subsaturating concentrations of macro- and micronutrients; increased surface area-to-volume ratios and narrower diffusional layer thickness combine to greatly increase nutrient acquisition capabilities (Gavis 1976; Wells 2003). However, a comparison of the uptake affinities for reduced nitrogen substrates (ammonium and urea) by cultured isolates of *P. cuspidata* (Auro 2007) relative to the larger-cell-sized species *P. australis* (Cochlan et al. 2008) and *P. multiseries* (Radan 2008) does not consistently indicate greater affinities for reduced N substrates by *P. cuspidata*. The ability of small cells such as *P.* cf. *delicatissima* to take up pulses of ammonium at initially elevated ("surge") uptake rates that greatly exceed their growth requirements (Auro 2007), a capability that is severely reduced in *P. multiseries* (Radan 2008), may provide the smaller cells with a competitive advantage over the larger-cell-sized species of *Pseudo-nitzschia* in areas and times of nitrogen limitation. Additionally, this greater ability to acquire these reduced nitrogen substrates, despite their generally very low ambient concentrations in the study area, provides them with additional nitrogenous sources for growth that are energetically less expensive for assimilation than nitrate (i.e., requiring both less reducing power and iron; Raven 1990; Cochlan et al. 2002).

In addition to the considerations of macronutrient uptake, a laboratory addition experiment at a location on the outer region of the Juan de Fuca eddy demonstrated iron limitation (Wells et al. 2005). Diatoms of the *Pseudo-nitzschia* genus have been shown to possess an inducible high affinity iron uptake capability that makes them particularly well adapted to grow on chelated iron forms relative to other coastal diatoms. This iron uptake capability would be further improved by the combination of high ratios of surface area to volume and higher diffusivity in the cellular boundary layers associated with smaller cell size (Wells 2003). Shifts between large and smaller *Pseudo-nitzschia* species might then be partly due to the substantial competitive advantage that small size would impart for iron uptake.

Association of Pseudo-nitzschia *blooms with specific phytoplankton assemblages*—In both the eddy and the nearshore regions, *Pseudo-nitzschia* typically were a member of mixed diatom assemblages. However, in the eddy, *Pseudo-nitzschia* also achieved high abundance as well as high toxicity during a dinoflagellate bloom (*Ceratium* and *Prorocentrum* spp.; September 2003; Table 3) and a euglenoid bloom (*Eutreptiella* sp.; September 2004). A nontoxic *Pseudo-nitzschia* bloom was observed during a bloom dominated by the dinoflagellate *Cochlodinium polykrikoides* at a nearshore station (GH02) influenced by a northward Columbia River plume (30 September 2006). Over all cruises, the abundance of *Pseudo-nitzschia* was significantly correlated with the combined abundance of *Ceratium* and *Prorocentrum* spp. (Olson et al. 2008), suggesting that this is a common association. Indeed, *Pseudo-nitzschia* has been reported to co-occur in a *Prorocentrum* bloom in Los Angeles harbor (Schnetzer et al. 2007). As *Pseudo-nitzschia* can thrive in conditions that favor either flagellate or diatom blooms, this genus is capable of succeeding in a wider range of habitats than most other diatoms. The eddy region appears to provide

the range of habitats that *Pseudo-nitzschia* can successfully exploit.

Relationship of environmental factors with toxic Pseudo-nitzschia *blooms in the Pacific Northwest*—Consistent with past studies using cultured *Pseudo-nitzschia* species where toxin production may increase under phosphate or silicic acid limitation (Bates et al. 1991; Pan et al. 1996*a*,*b*; Fehling et al. 2004), field studies of recent blooms of *P. australis* in southern California have reported significant negative correlations between both pDA and *Pseudo-nitzschia* concentrations and the ambient concentrations of $Si(OH)_4$, NO_3^- (or $NO_3^- + NO_2^-$) (Anderson et al. 2006; Schnetzer et al. 2007), or PO_4^{3-} (Schnetzer et al. 2007). These negative relationships, coupled with significant negative correlations between pDA and the elemental ratios of $Si(OH)_4 : PO_4^{3-}$ and $NO_3^- : PO_4^{3-}$ (Anderson et al. 2006) and $Si(OH)_4 : PO_4^{3-}$ and $NO_3^- : PO_4^{3-}$, but not $NO_3^- : Si(OH)_4$ (Schnetzer et al. 2007), have led to the speculation that both absolute concentrations of these specific elements and elemental ratios play a role in the development of blooms of *P. australis* and DA production. However, these authors also suggest that such negative correlations with macronutrients may be a result merely of their drawdown during the development of the toxic diatom blooms. Our results, obtained with over 550 surface samples over 4 yr, including six cruises, showed no correlation of *Pseudo-nitzschia* or pDA concentrations to macronutrient concentrations when the entire sampling grid was considered (Table 4), in agreement with similar regression analyses conducted previously by Marchetti et al. (2004) for the Juan de Fuca eddy region and coastal waters of Washington State and British Columbia. Although significant ($p < 0.05$) positive relationships between pDA and the elemental ratios of both $NO_3^- : PO_4^{3-}$ and $Si(OH)_4 : PO_4^{3-}$ in the eddy region are suggestive of a potential role of PO_4^{3-} stress in pDA production, absolute concentrations of PO_4^{3-} were never reduced to levels considered limiting for the growth of diatoms in this region, and thus such ratios need to be interpreted with caution.

When the eddy and nearshore regions were considered separately (not shown), weak but significant relationships between macronutrients and pDA were observed (<25% of the variance explained), positive for the eddy region and negative for the nearshore zone. The negative relationship found in the nearshore zone is consistent with the result that most nearshore stations where pDA was observed were in nutrient-depleted downwelling or Columbia River plume waters close to the river mouth. The positive relationship found in the eddy region indicates that pDA was generally found in nutrient-replete upwelled or estuarine waters. Thus, *Pseudo-nitzschia* spp. produce DA in this region under both nitrate- and silicic acid–replete or depleted conditions, indicating that macronutrient stress is not a strong determinant for toxicity for natural assemblages in the Pacific Northwest, in contrast to what has been suggested for other regions (Anderson et al. 2006).

In general, we find significant ($p < 0.05$) positive relationships between pDA and *Pseudo-nitzschia* cell concentrations, but on numerous occasions pDA was undetectable or low despite moderate to high densities of *Pseudo-nitzschia* (Table 2), an observation that has also been made in California coastal waters (Trainer et al. 2000). A significant positive relationship was observed between concentrations of Chl *a* and *Pseudo-nitzschia* over the whole grid (Table 4). This relationship held even when September 2004 bloom data were removed from the analysis ($r_s = 0.52^{**}$, $n = 478$) but was much stronger when just September 2004 data were considered ($r_s = 0.72^{**}$, $n = 83$). Significant relationships also existed between Chl *a* and pDA over the entire sampling grid and in the eddy region but were substantially weaker compared to the relationship between Chl *a* and *Pseudo-nitzschia* (Table 4; Fig. 7). Remotely sensed images of Chl *a* may therefore indicate the presence of *Pseudo-nitzschia* cells in the years sampled but cannot specify whether those *Pseudo-nitzschia* species are producing DA. Also, within the nearshore zone where DA accumulates in recreationally harvested razor clams and other commercially harvested benthic organisms, no significant relationship between Chl *a* and pDA was observed (Table 4). Even when high abundances of *Pseudo-nitzschia* spp. were observed in the nearshore zone (e.g., 1×10^6 cells L^{-1} at GH01 on 14 September 2005; Table 3), *Pseudo-nitzschia* spp. never dominated the phytoplankton community biomass (Table 3). Therefore, *Pseudo-nitzschia* spp. are unlikely to be the phytoplankton responsible for increases in remotely sensed Chl *a* biomass found near the coast. These severe biological limitations, coupled with the fact that only about 5% of imagery in the eddy region is cloud free during summer months (based on 10 yr of data; K. Edwards and B. Hickey unpubl.), show that remote sensing of chlorophyll will be ineffective for real-time forecasting of toxigenic *Pseudo-nitzschia* blooms in the Pacific Northwest.

When the entire grid is considered, correlations between pDA and *Pseudo-nitzschia* cell numbers and temperature and salinity were either not significant or extremely weak (temperature only) (Table 4). There appears to be a window of particular water properties favorable to high values of pDA, namely, temperatures of 11–15°C and salinities of 31.5–33.0 (Fig. 7). These ranges suggest pDA is rarely found in recently upwelled bottom water, whose temperature is generally ~ 8°C, though we cannot rule out that these waters carry the seed populations of *Pseudo-nitzschia*. Relationships between pDA and temperature and salinity improve slightly when regions are considered separately, with opposite correlations in the eddy and nearshore regions. In particular, higher pDA is related to colder, saltier, and more nutrient-rich water in the eddy as well as warmer, fresher, and lower-nutrient waters in the nearshore region. The latter indicated that the higher values of pDA in the nearshore region were most frequently not related to recently upwelled coastal water, suggesting that they may have originated from the eddy. Although pDA was sometimes observed near the edges of the Columbia River plume, whether the toxin is produced in situ in plume water is presently unknown. However, toxic cells from offshore may be entrained into Columbia River water and then transported northward within the plume (Adams et al. 2006).

Even though we identify some significant relationships in our correlation analysis, none can be used consistently to predict with any confidence the occurrence of toxic blooms of *Pseudo-nitzschia* spp. in the nearshore zone where they threaten human health by consumption of contaminated shellfish. It is possible that a sequence or combination of environmental factors could be useful for prediction.

References

Adams, N. G., M. Lesoing, and V. L. Trainer. 2000. Environmental conditions associated with domoic acid in razor clams on the Washington coast. J. Shellfish Res. **19:** 1007–1015.

———, A. MacFadyen, B. M. Hickey, and V. L. Trainer. 2006. The nearshore advection of a toxigenic *Pseudo-nitzschia* bloom and subsequent domoic acid contamination of intertidal bivalves. Afr. J. Mar. Sci. **28:** 271–276.

Anderson, C. R., M. A. Brzezinski, L. Washburn, and R. Kudela. 2006. Circulation and environmental conditions during a toxigenic *Pseudo-nitzschia australis* bloom in the Santa Barbara Channel, California. Mar. Ecol. Prog. Ser. **327:** 119–133.

Auro, M. E. 2007. Nitrogen dynamics and toxicity of the pennate diatom *Pseudo-nitzschia cuspidata*: A field and laboratory study. M.S. thesis. San Francisco State Univ.

Bates, S. S., A. S. W. de Frietas, J. E. Milley, R. Pocklington, M. A. Quilliam, J. C. Smith, and J. Worms. 1991. Controls on domoic acid production by the diatom *Nitzschia pungens* f. *multiseries* in culture: Nutrients and irradiance. Can. J. Fish. Aquat. Sci. **48:** 1136–1144.

Baugh, K. A., J. M. Bush, B. D. Bill, K. A. Lefebvre, and V. L. Trainer. 2006. Estimates of specific toxicity in several *Pseudo-nitzschia* species from the Washington coast, based on culture and field studies. Afr. J. Mar. Sci. **28:** 403–407.

———, S. G. Spencer, J. C. Wekell, and V. L. Trainer. 2004. An alternative method for domoic acid determination in seawater particulates: a receptor-binding assay using glutamate dehydrogenase, p. 228–230. *In* K. A. Steidinger, J. H. Landsberg, C. R. Tomas and G. A. Vargo [eds.], Harmful algae 2002. Florida Fish and Wildlife Commission, Florida Institute of Oceanography, Intergovernmental Oceanographic Commission of UNESCO.

Bill, B. D., F. H. Cox, R. A. Horner, J. A. Borchert, and V. L. Trainer. 2006. The first closure of shellfish harvesting due to domoic acid in Puget Sound, Washington, USA. Afr. J. Mar. Sci. **28:** 437–442.

Cochlan, W. P., D. A. Bronk, and K. H. Coale. 2002. Trace metals and nitrogenous nutrition of Antarctic phytoplankton: Experimental observations in the Ross Sea. Deep-Sea Res. II **49:** 3365–3390.

———, J. Herndon, and R. M. Kudela. 2008. Inorganic and organic nitrogen uptake by the toxigenic diatom *Pseudo-nitzschia australis* (Bacillariophyceae). Harmful Algae. doi:10.1016/j.hal.2008.08.008.

Fehling, J., K. Davidson, C. J. Bolch, and S. S. Bates. 2004. Growth and domoic acid production by *Pseudo-nitzschia seriata* (Bacillariophyceae) under phosphate and silicate limitation. J. Phycol. **40:** 674–683.

Foreman, M. G. G., W. Callendar, A. MacFadyen, B. M. Hickey, R. E. Thomson, and E. Di Lorenzo. 2008. Modeling the generation of the Juan de Fuca eddy. J. Geophys. Res. Oceans **113:** C03006, doi:10.1029/2006JC004082.

Freeland, H. J., and K. L. Denman. 1982. A topographically controlled upwelling center off southern Vancouver Island. J. Mar. Res. **40:** 1069–1093.

Gavis, J. 1976. Munk and Riley revisited: Nutrient diffusion transport and rates of phytoplankton growth. J. Mar. Sci. **34:** 161–179.

Hickey, B. M. 1989. Patterns and processes of shelf and slope circulation, p. 41–115. *In* M. R. Landry and B. M. Hickey [eds.], Coastal oceanography of Washington and Oregon. Elsevier Science.

———, and N. Banas. 2003. Oceanography of the Pacific Northwest Coastal Ocean and estuaries with application to coastal ecosystems. Estuaries **26:** 1010–1031.

———, S. Geier, N. Kachel, and A. MacFadyen. 2005. A bi-directional river plume: The Columbia in summer. Cont. Shelf Res. **25:** 1631–1636.

———, A. MacFadyen, W. Cochlan, R. Kudela, K. Bruland, and C. Trick. 2006. Evolution of chemical, biological, and physical water properties in the northern California Current in 2005. Geophys. Res. Lett. **33:** L22S02, doi:10.1029/2006GL026782.

Howard, M. D. A., W. P. Cochlan, N. Ladizinsky, and R. M. Kudela. 2007. Nitrogenous preference of toxigenic *Pseudo-nitzschia australis* (Bacillariophyceae) from field and laboratory experiments. Harmful Algae **6:** 206–217.

Knepel, K., and K. Bogren. 2002. Determination of orthophosphate by flow injection analysis: QuikChem® Method 31-115-01-1-H, p. 14. Lachat Instruments.

Lessard, E. J., and M. C. Murrell. 1996. Distribution, abundance and size composition of heterotrophic dinoflagellates and ciliates in the Sargasso Sea near Bermuda. Deep-Sea Res. I **43:** 1045–1065.

Lundholm, N., P. J. Hansen, and Y. Kotaki. 2004. Effect of pH on growth and domoic acid production by potentially toxic diatoms of the genera *Pseudo-nitzschia* and *Nitzschia*. Mar. Ecol. Prog. Ser. **273:** 1–15.

———, Ø. Moestrup, G. R. Hasle, and K. Hoef-Emden. 2003. A study of the *Pseudo-nitzschia pseudodelicatissima/cuspidata* complex (Bacillariophyceae): What is a *P. pseudodelicatissima*? J. Phycol **39:** 797–813.

MacFadyen, A., B. M. Hickey, and W. P. Cochlan. 2008. Influences of the Juan de Fuca eddy on circulation, nutrients and phytoplankton production in the northern California Current System. J. Geophys. Res. **113:** C08008, doi:10.1029/2007JC004412.

———, B. M. Hickey, and M. G. G. Foreman. 2005. Transport of surface waters from the Juan de Fuca eddy region to the Washington coast. Cont. Shelf Res. **25:** 2008–2021.

Mackas, D. L., G. C. Loutitt, and M. J. Austin. 1980. Spatial distribution of zooplankton and phytoplankton in British Columbian coastal waters. Can. J. Fish. Aquat. Sci. **37:** 1476–1487.

Maldonado, M. T., M. Hughes, E. Rue, and M. L. Wells. 2002. The effect of Fe and Cu on the growth and domoic acid production of *Pseudo-nitzschia multiseries* and *Pseudo-nitzschia australis*. Limnol. Oceanogr. **47:** 515–526.

Marchetti, A., V. L. Trainer, and P. J. Harrison. 2004. Environmental conditions and phytoplankton dynamics associated with *Pseudo-nitzschia* abundance and domoic acid in the Juan de Fuca eddy. Mar. Ecol. Prog. Ser. **281:** 1–12.

Menden-Deuer, S., and E. J. Lessard. 2000. Carbon to volume relationships for dinoflagellates, diatoms, and other protist plankton. Limnol. Oceanogr. **45:** 569–579.

Olson, M. B., E. J. Lessard, W. P. Cochlan, and V. L. Trainer. 2008. Intrinsic growth and microzooplankton grazing on toxigenic *Pseudo-nitzschia* diatoms from the Pacific Northwest, USA. Limnol. Oceanogr. **53:** 1352–1368.

———, ———, C. H. J. Wong, and M. J. Bernhardt. 2006. Copepod feeding selectivity on microplankton, including the toxigenic diatoms *Pseudo-nitzschia* spp., in the coastal Pacific Northwest. Mar. Ecol. Prog. Ser. **326:** 207–220.

O'Reilly, J. E., and others. 2000. Ocean chlorophyll a algorithms for SeaWiFS, OC2, and OC4: Version 4. p. 9–19. *In* J. E. O'Reilly and 24 coauthors, SeaWiFS postlaunch calibration and validation analyses, part 3. NASA Tech. Memo 2000-206892, **11:** 9–19.

Pan, Y., D. V. S. Rao, and K. H. Mann. 1996*a*. Changes in domoic acid production and cellular chemical composition of the toxigenic diatom *Pseudo-nitzschia multiseries* under phosphate limitation. J. Phycol. **32:** 371–381.

———, ———, ———, W. K. W. Li, and W. G. Harrison. 1996*b*. Effects of silicate limitation on production of domoic acid, a neurotoxin, by the diatom *Pseudo-nitzschia multiseries*. II. Continuous culture studies. Mar. Ecol. Prog. Ser. **131:** 235–243.

Parsons, T. R., Y. Maita, and C. M. Lalli. 1984. A manual of chemical and biological methods for seawater analysis. Pergamon Press.

Radan, R. L. 2008. Nitrogen uptake and domoic acid production by the toxigenic diatom *Pseudo-nitzschia multiseries*. M.S. thesis. San Francisco State Univ.

Raven, J. A. 1990. Predictions of Mn and Fe use efficiencies of phototrophic growth as a function of light availability for growth and of C assimilation pathway. New Phytol. **116:** 1–18.

Roff, J. C., and R. R. Hopcroft. 1986. High precision microcomputer based measuring system for ecological research. Can. J. Fish. Aquat. Sci. **43:** 2044–2048.

Rue, E., and K. W. Bruland. 2001. Domoic acid binds iron and copper: A possible role for the toxin produced by the marine diatom *Pseudo-nitzschia*. Mar. Chem. **76:** 127–134.

Schnetzer, A., and others. 2007. Blooms of *Pseudo-nitzschia* and domoic acid in the San Pedro Channel and Los Angeles harbor areas of the Southern California Bight, 2003–2004. Harmful Algae **6:** 372–387.

Scholin, C. A., and others. 2000. Mortality of sea lions along the central California coast linked to a toxic diatom bloom. Nature **403:** 80–84.

Smith, P., and K. Bogren. 2001. Determination of nitrate and/or nitrite in brackish or seawater by flow injection analysis colorimeter: QuickChem Method 31-107-04-1-E, p. 12. Lachat Instruments.

Stehr, C. M., L. Connell, K. A. Baugh, B. D. Bill, N. G. Adams, and V. L. Trainer. 2002. Morphological, toxicological, and genetic differences among *Pseudo-nitzschia* (Bacillariophyceae) species in inland embayments and outer coastal waters of Washington State, USA. J. Phycol. **38:** 55–65.

Stumpf, R. P., R. A. Arnone, R. W. Gould, P. Martinolich, and V. Ransibrahmanakul. 2003. A partially coupled ocean-atmosphere model for retrieval of water-leaving radiance from SeaWiFS in coastal waters, p. 51–59. *In* S. B. Hooker and E. R. Firestone [eds.], Algorithm updates for the fourth SeaWiFS data processing. SeaWiFS Postlaunch Technical Report Series, vol. 20.

Trainer, V. L., N. G. Adams, and J. C. Wekell. 2001. Domoic acid-producing *Pseudo-nitzschia* species off the U.S. west coast associated with toxification events, p. 46–48. *In* G. M. Hallegraeff, S. I. Blackburn, C. J. Bolch and R. J. Lewis [eds.], Proceedings of the ninth international conference on harmful algal blooms. Intergovernmental Oceanographic Commission of UNESCO.

———, B. M. Hickey, and R. A. Horner. 2002. Biological and physical dynamics of domoic acid production off the Washington U.S.A. coast. Limnol. Oceanogr. **47:** 1438–1446.

———, and M. Suddleson. 2005. Monitoring approaches for early warning of domoic acid events in Washington State. Oceanography **18:** 228–237.

———, and others. 2000. Domoic acid production near California upwelling zones, June 1998. Limnol. Oceanogr. **45:** 401–440.

Washington State Department of Health. 2007. Office of Shellfish and Water Protection 2006 annual inventory of commercial and recreational shellfish areas in Washington State.

Wekell, J. C., E. J. Gauglitz Jr., H. J. Barnett, C. L. Hatfield, D. Simons, and D. Ayres. 1994. Occurrence of domoic acid in Washington state razor clams (*Siliqua patula*) during 1991–1993. Nat. Toxins **2:** 197–205.

Wells, M. L. 2003. The level of iron enrichment required to initiate diatom blooms in HNLC waters. Mar. Chem. **82:** 101–114.

———, C. G. Trick, W. P. Cochlan, M. P. Hughes, and V. L. Trainer. 2005. Domoic acid: The synergy of iron, copper, and the toxicity of diatoms. Limnol. Oceanogr. **50:** 1908–1917.

Welschmeyer, N. A. 1994. Fluorometric analysis of chlorophyll-*a* in the presence of chlorophyll-*b* and phaeopigments. Limnol. Oceanogr. **39:** 1985–1992.

Wolters, M. 2002. Determination of silicate in brackish or seawater by flow injection analysis.QuikChem® Method 31-114-27-1-D, p. 12. Lachat Instruments.

Worden, A., J. K. Nolan, and B. Palenik. 2004. Assessing the dynamics and ecology of marine picophytoplankton: the importance of the eukaryotic component. Limnol. Oceanogr. **49:** 168–179.

Work, T. M., B. Barr, A. M. Beale, L. Fritz, M. A. Quilliam, and J. L. C. Wright. 1993. Epidemiology of DA poisoning in brown pelicans (*Pelecanus occidentalis*) and Brandt's cormorants (*Phalacrocarax penicillatus*) in California. J. Zoo Wildl. Med. **24:** 54–62.

Wright, J. L. C., and others. 1989. Identification of domoic acid, a neuroexcitatory amino acid, in toxic mussels from eastern Prince Edward Island. Can. J. Chem. **67:** 481–490.

Edited by: Roland Psenner

Received: 1 February 2008
Accepted: 21 June 2008
Amended: 8 August 2008